The QCD Equation of State to $O(\mu_B^6)$

Prasad Hegde
Center for High Energy Physics,
Indian Institute of Science, Bangalore

For the Bielefeld-BNL-CCNU collaboration

23rd June 2017

The 35th International Symposium on Lattice Field Theory (Lattice 2017)
Palacio de Congresos de Granada,
Granada, Spain.

Bielefeld-BNL-CCNU collaboration

A. Bazavov (Michigan State U.)

H.-T. Ding (CCNU)

P. Hegde (IISc)

O. Kaczmarek (Bielefeld U./CCNU)

F. Karsch (Bielefeld U./BNL)

E. Laermann (Bielefeld U.)

Y. Maezawa (YITP)

S. Mukherjee (BNL)

H. Ohno (U. Tsukuba/BNL)

P. Petreczky (BNL)

H. Sandmeyer (Bielefeld U.)

C. Schmidt (Bielefeld U.)

S. Sharma (BNL)

W. Soeldner (Regensburg U.)

P. Steinbrecher (Bielefeld U./BNL)

M. Wagner (NVIDIA)

QCD at finite density

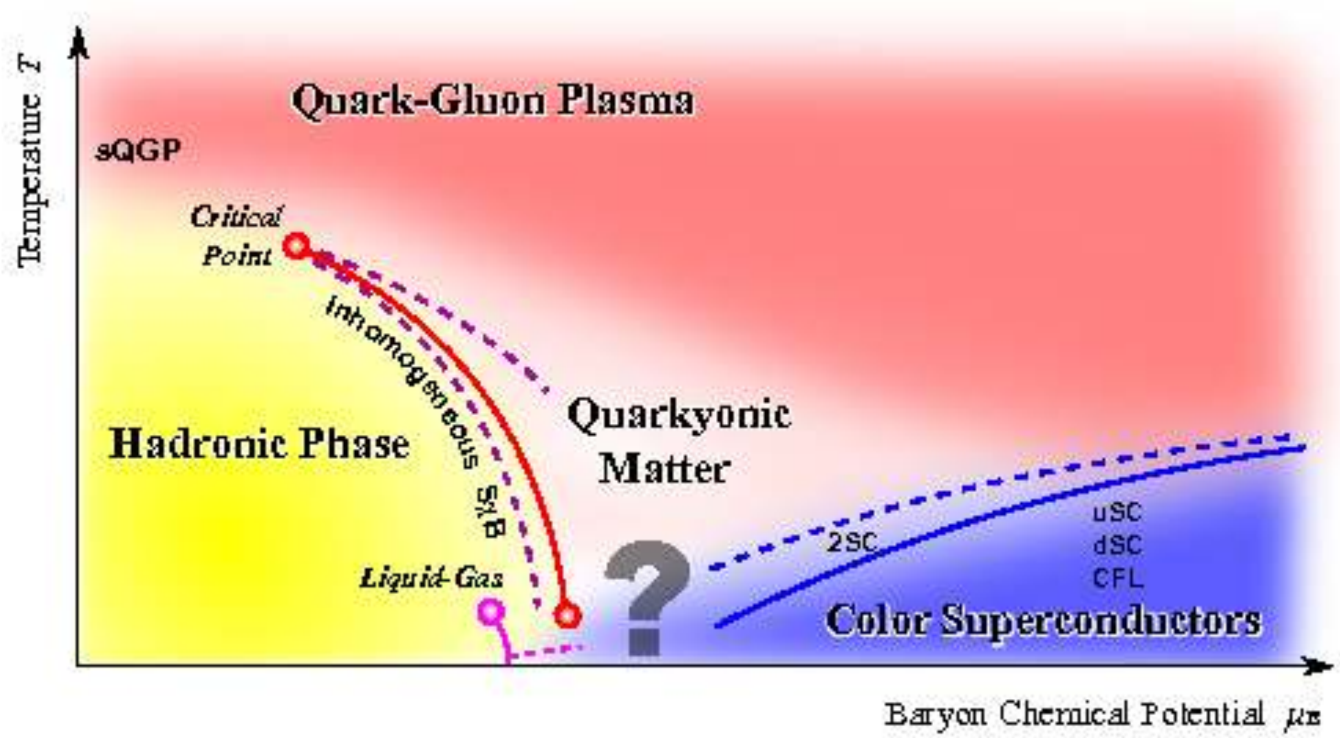

Ordinary nuclear matter: μ_B ~ 940 MeV and T ~ 0K.
Rest of the diagram virtually unknown.

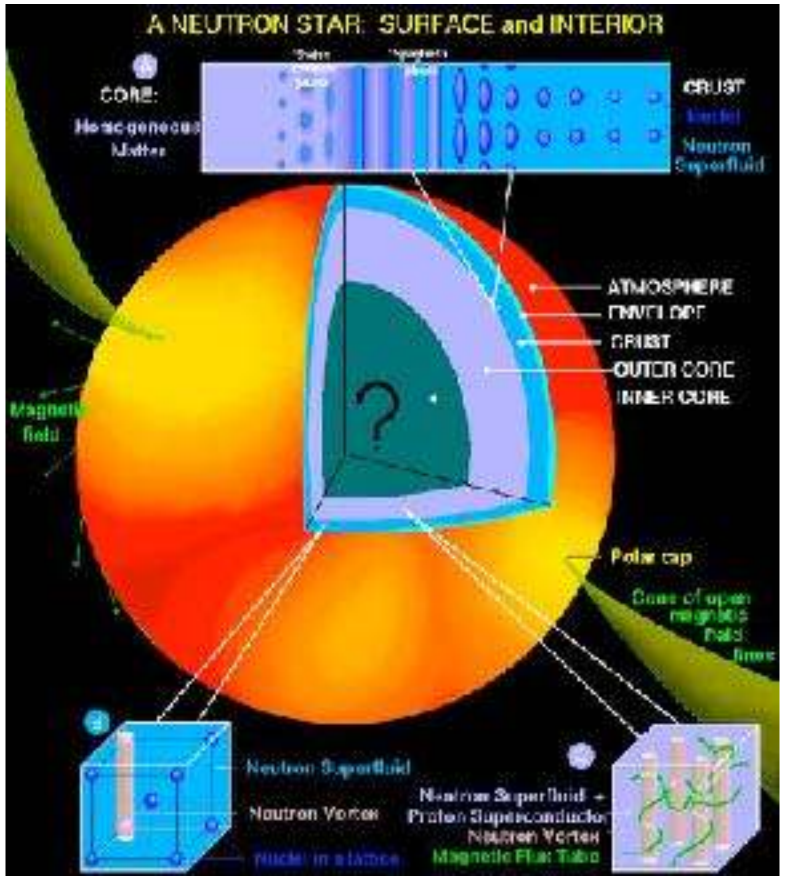

Dense nuclear matter can be found in nature, in the interiors (and surface) of neutron stars for e.g.

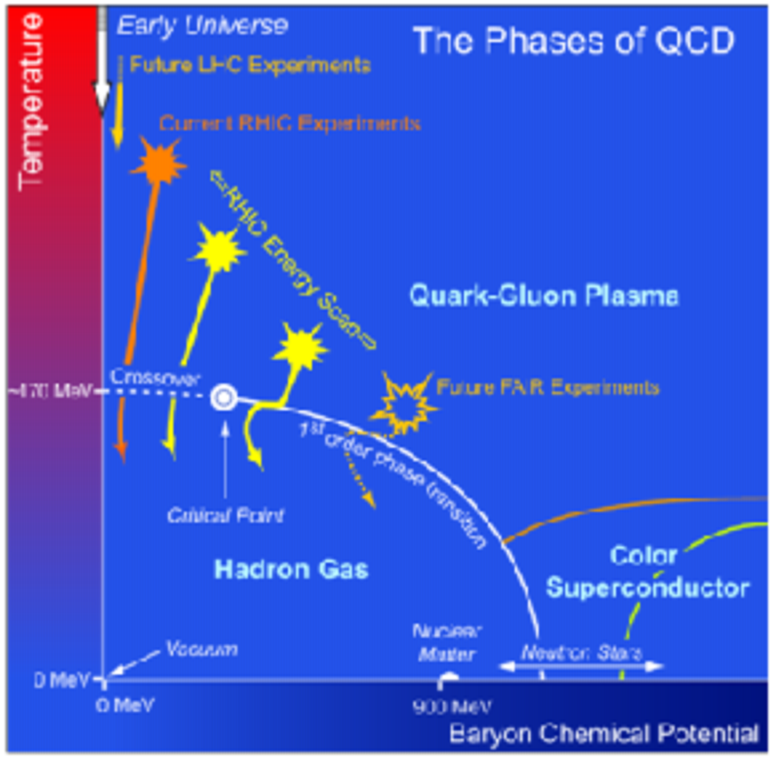

Some parts of this phase diagram will be explored at RHIC, as well as at FAIR, NICA & J-PARC in the future.

Beam Energy Scan and the QCD Critical Point

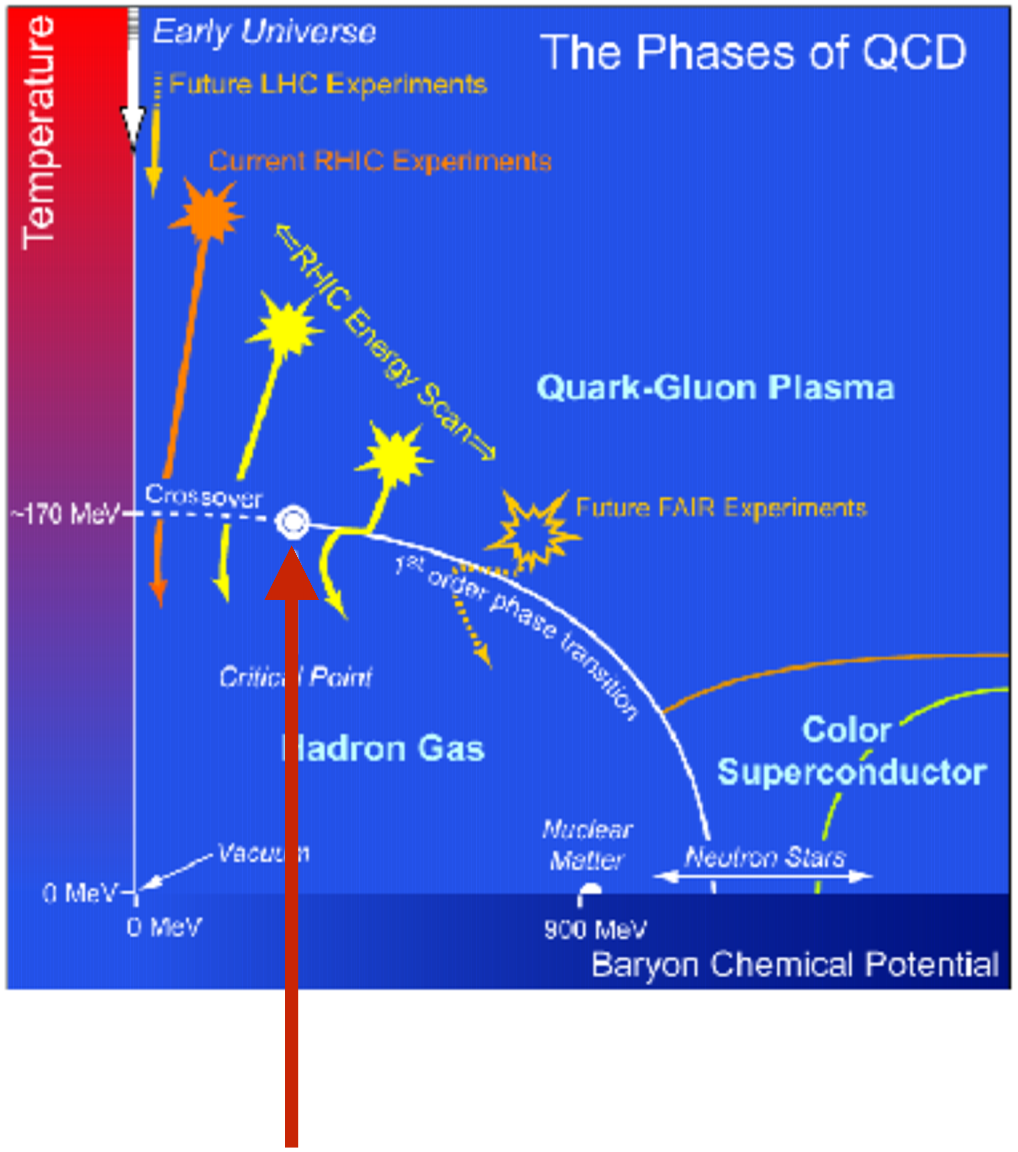

The Beam Energy Scan (BES) program at RHIC was designed to look for the conjectured QCD critical point.

The collision energy of the heavy ions is to be varied from the top RHIC energy of 200A-GeV down to about 5.5A-GeV.

The hadrons formed in a lower energy collision have a higher baryochemical potential μ_B at freezeout.

If a critical point exists, then the evolution of the fireball created in these collisions should be qualitatively different in the first order region than in the crossover region.

Need to validate any experimental observation from theory. Some theoretical estimates place the critical point at μ_B/T ~ 1.5-2 while others place it much higher.

Calculating at finite density

- Models (PNJL, large-N_c, etc.): Possible to calculate an equation of state even for large densities, as well as putative phase diagrams. However, results will necessarily be qualitative or semi-quantitative.

- **Lattice QCD:** *Ab initio,* but afflicted by the sign problem. Several partial solutions known, but only two have been applied to large-scale QCD calculations:

  - Imaginary-μ: No sign problem at imaginary μ; however an analytic continuation is required back to real μ. [J. Gunther et al. EPJ Webconf 137 07008 (2017); D'Elia et al. Phys Rev. D95, no 9., 094503 (2017); talks by J. Gunther and A. Pasztor earlier today].

  - Method of Taylor expansions [Gavai-Gupta (TIFR) (2002), Allton et al. (RBC-Bielefeld) (2003)]: Straightforward definition. However, signal-to-noise ratio falls quickly with increasing order and large volumes.

The method of Taylor expansions

- The quark number susceptibilities (QNS) are the Taylor coefficients of the expansion of the pressure i.e. logarithm of the partition function, w.r.t. the chemical potential μ.

$$\chi_{ijk}^{BQS} = \left[\frac{\partial^{i+j+k}}{\partial \hat{\mu}_B^i \partial \hat{\mu}_Q^j \partial \hat{\mu}_S^k} \left(\frac{p}{T^4} \right) \right]_{\mu_B=\mu_Q=\mu_S=0} \qquad (\hat{\mu} \equiv \mu/T)$$

- To calculate these on the lattice, it is necessary to take derivatives of the quark matrix e.g.

$$\begin{aligned}
\frac{\partial^6 \ln \det M}{\partial \mu^6} = {} & \mathrm{Tr}\left(M^{-1}\frac{\partial^6 M}{\partial \mu^6}\right) - 6\,\mathrm{Tr}\left(M^{-1}\frac{\partial M}{\partial \mu}M^{-1}\frac{\partial^5 M}{\partial \mu^5}\right) - 15\,\mathrm{Tr}\left(M^{-1}\frac{\partial^2 M}{\partial \mu^2}M^{-1}\frac{\partial^4 M}{\partial \mu^4}\right) - 10\,\mathrm{Tr}\left(M^{-1}\frac{\partial^3 M}{\partial \mu^3}M^{-1}\frac{\partial^3 M}{\partial \mu^3}\right) \\
& + 30\,\mathrm{Tr}\left(M^{-1}\frac{\partial M}{\partial \mu}M^{-1}\frac{\partial M}{\partial \mu}M^{-1}\frac{\partial^4 M}{\partial \mu^4}\right) + 60\,\mathrm{Tr}\left(M^{-1}\frac{\partial M}{\partial \mu}M^{-1}\frac{\partial^2 M}{\partial \mu^2}M^{-1}\frac{\partial^3 M}{\partial \mu^3}\right) \\
& + 60\,\mathrm{Tr}\left(M^{-1}\frac{\partial^2 M}{\partial \mu^2}M^{-1}\frac{\partial M}{\partial \mu}M^{-1}\frac{\partial^3 M}{\partial \mu^3}\right) + 30\,\mathrm{Tr}\left(M^{-1}\frac{\partial^2 M}{\partial \mu^2}M^{-1}\frac{\partial^2 M}{\partial \mu^2}M^{-1}\frac{\partial^2 M}{\partial \mu^2}\right) \\
& - 120\,\mathrm{Tr}\left(M^{-1}\frac{\partial M}{\partial \mu}M^{-1}\frac{\partial M}{\partial \mu}M^{-1}\frac{\partial M}{\partial \mu}M^{-1}\frac{\partial^3 M}{\partial \mu^3}\right) - 180\,\mathrm{Tr}\left(M^{-1}\frac{\partial M}{\partial \mu}M^{-1}\frac{\partial M}{\partial \mu}M^{-1}\frac{\partial^2 M}{\partial \mu^2}M^{-1}\frac{\partial^2 M}{\partial \mu^2}\right) \\
& - 90\,\mathrm{Tr}\left(M^{-1}\frac{\partial M}{\partial \mu}M^{-1}\frac{\partial^2 M}{\partial \mu^2}M^{-1}\frac{\partial M}{\partial \mu}M^{-1}\frac{\partial^2 M}{\partial \mu^2}\right) + 360\,\mathrm{Tr}\left(M^{-1}\frac{\partial M}{\partial \mu}M^{-1}\frac{\partial M}{\partial \mu}M^{-1}\frac{\partial M}{\partial \mu}M^{-1}\frac{\partial M}{\partial \mu}M^{-1}\frac{\partial^2 M}{\partial \mu^2}\right) \\
& - 120\,\mathrm{Tr}\left(M^{-1}\frac{\partial M}{\partial \mu}M^{-1}\frac{\partial M}{\partial \mu}M^{-1}\frac{\partial M}{\partial \mu}M^{-1}\frac{\partial M}{\partial \mu}M^{-1}\frac{\partial M}{\partial \mu}M^{-1}\frac{\partial M}{\partial \mu}\right).
\end{aligned}$$

The Method of Taylor Expansions (contd')

- These traces cannot be evaluated exactly, since M^{-1} cannot be evaluated exactly. They must be evaluated stochastically. In our case, we used 500 random vectors for the higher order traces and 1500 random vectors for the trace D_1 per configuration [Might be possible to use fewer vectors; see the poster by de Forcrand and Jaeger].

- After these traces are evaluated, they are put together in the necessary combination to calculate the relevant QNS's e.g.

$$\begin{aligned}\mathcal{A}_6 = &\langle\mathcal{D}_6\rangle + 6\langle\mathcal{D}_5\mathcal{D}_1\rangle + 15\langle\mathcal{D}_4\mathcal{D}_2\rangle + 10\langle\mathcal{D}_3^2\rangle \\ &+ 15\langle\mathcal{D}_4\mathcal{D}_1^2\rangle + 60\langle\mathcal{D}_3\mathcal{D}_2\mathcal{D}_1\rangle + 15\langle\mathcal{D}_2^3\rangle \\ &+ 20\langle\mathcal{D}_3\mathcal{D}_1^3\rangle + 45\langle\mathcal{D}_2^2\mathcal{D}_1^2\rangle + 15\langle\mathcal{D}_2\mathcal{D}_1^4\rangle + \langle\mathcal{D}_1^6\rangle.\end{aligned}$$

Here A_6 is the combination required to calculate χ_6. Care must be taken to evaluate the squares, cubes, etc. in an unbiased manner. Once this is done for each configuration, the QNS can be calculated by averaging over the ensemble.

- The signal-to-noise ratio drops quickly with increasing order. Need very high statistics in order to get a decent result for the higher order susceptibilities.

QCD at finite density

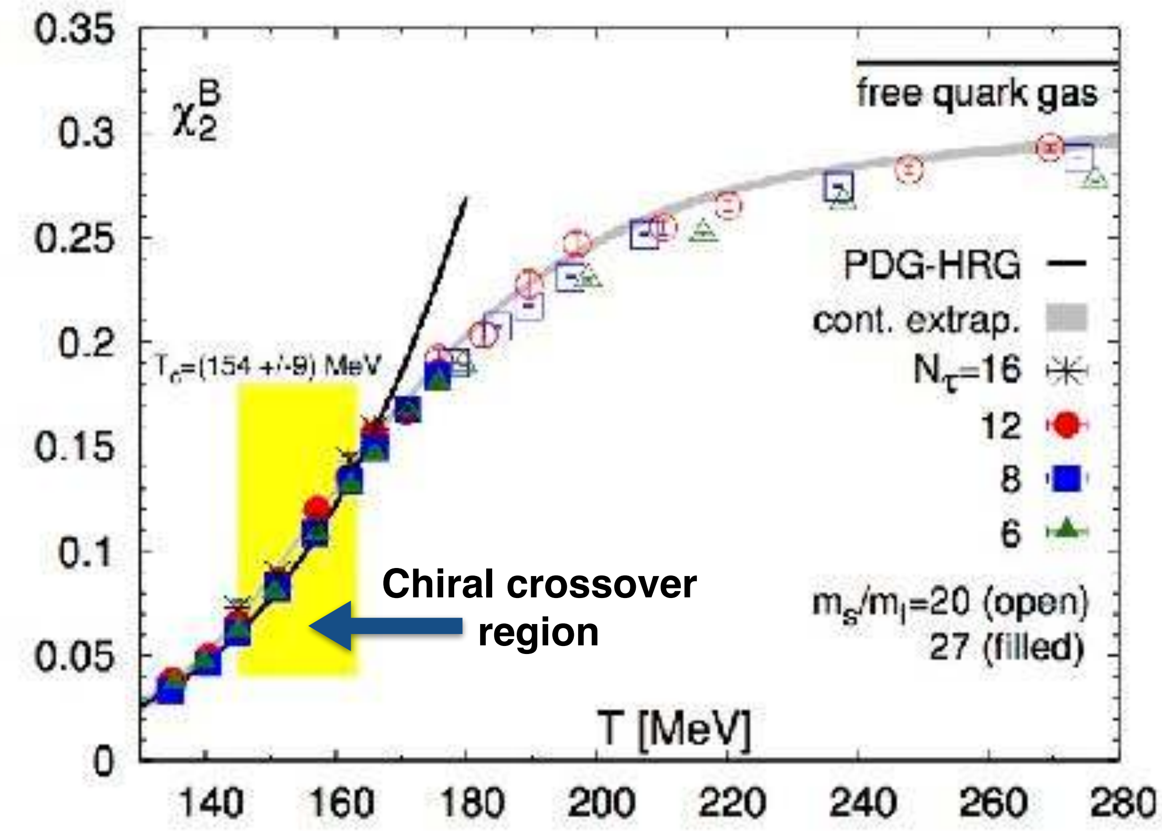

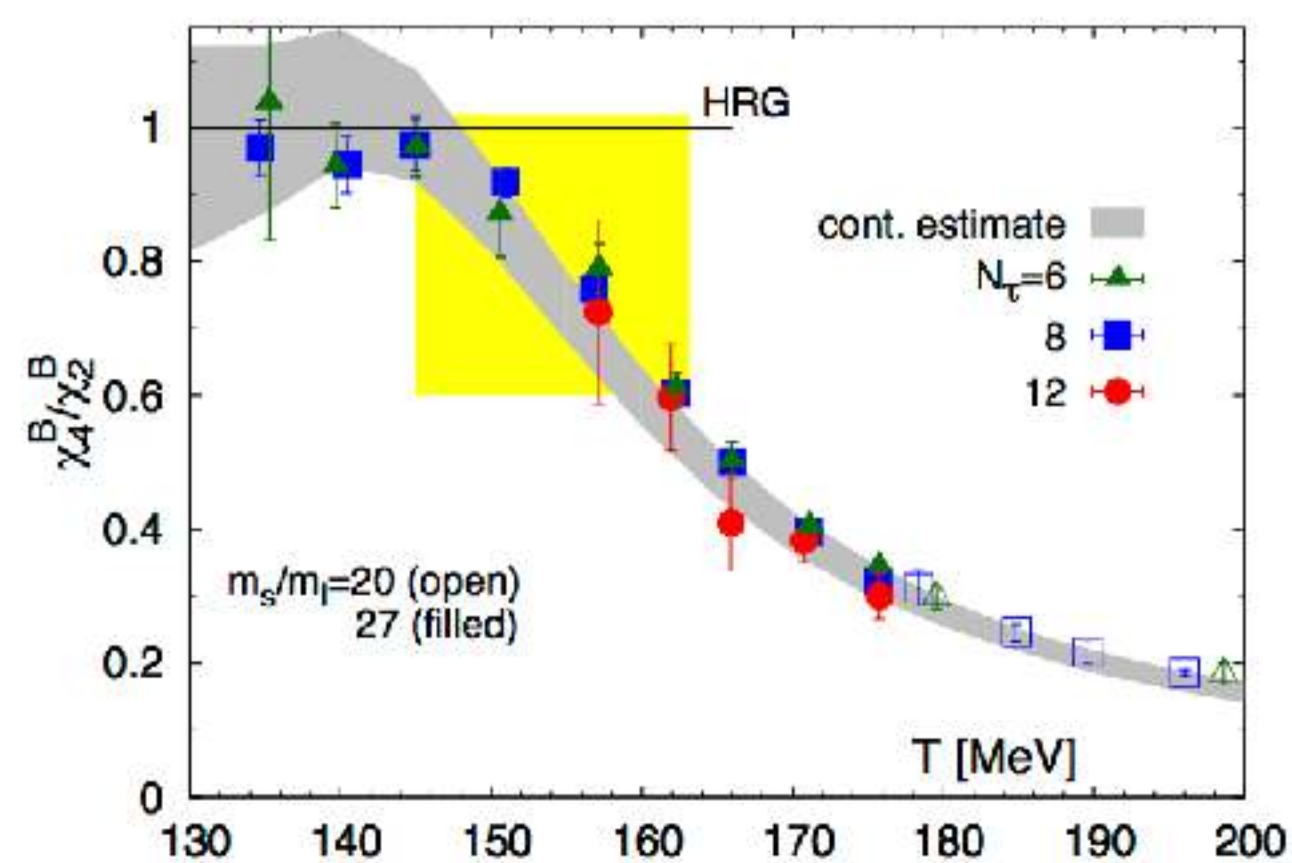

- We calculated all the QNS (49 in all) up to sixth order, on lattices of size 6 – 16, in the temperature range [135 MeV, 280 MeV] and for two quark masses viz. $m_l = m_s/20$ and $m_l = m_s/27$.
- Multiple lattice spacings allowed us to take the continuum limit in the 2^{nd} order case while for the 4^{th} and 6^{th} order cases, our high-statistics results for N_t = 6 & 8 allowed us to calculate the continuum estimate.

QCD at finite density

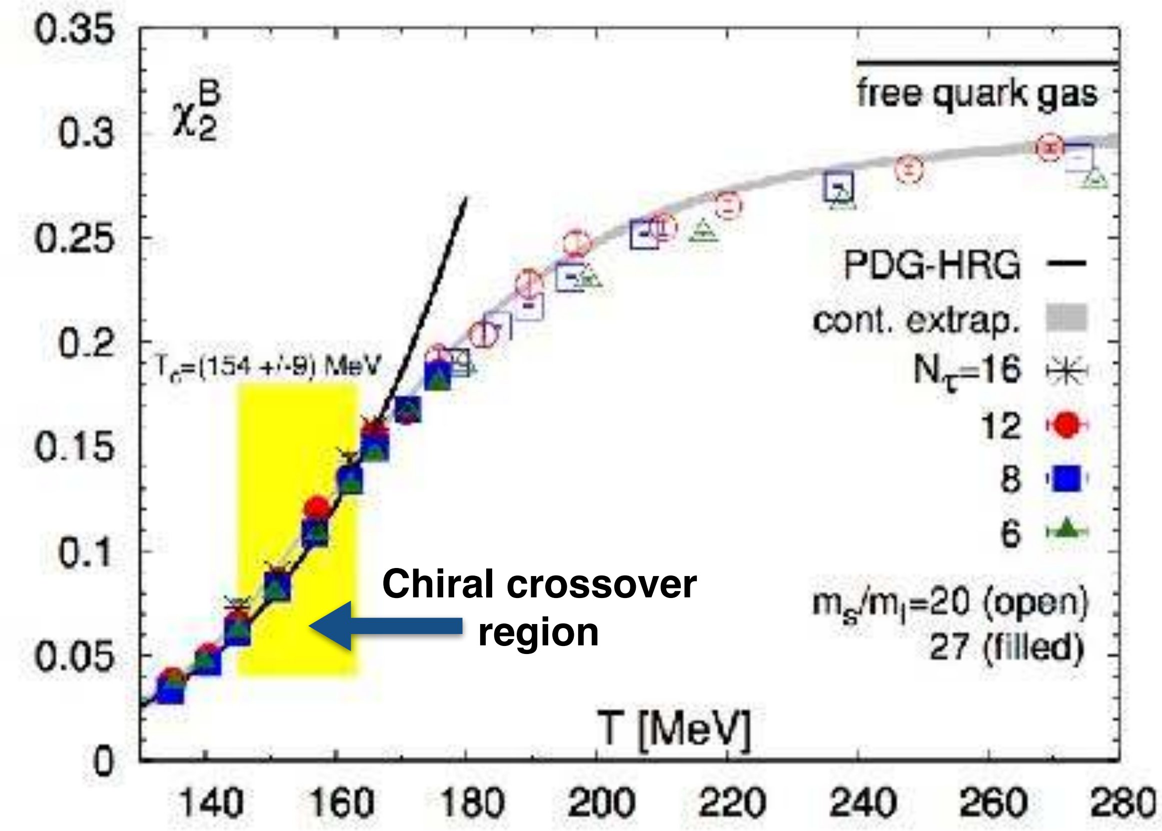

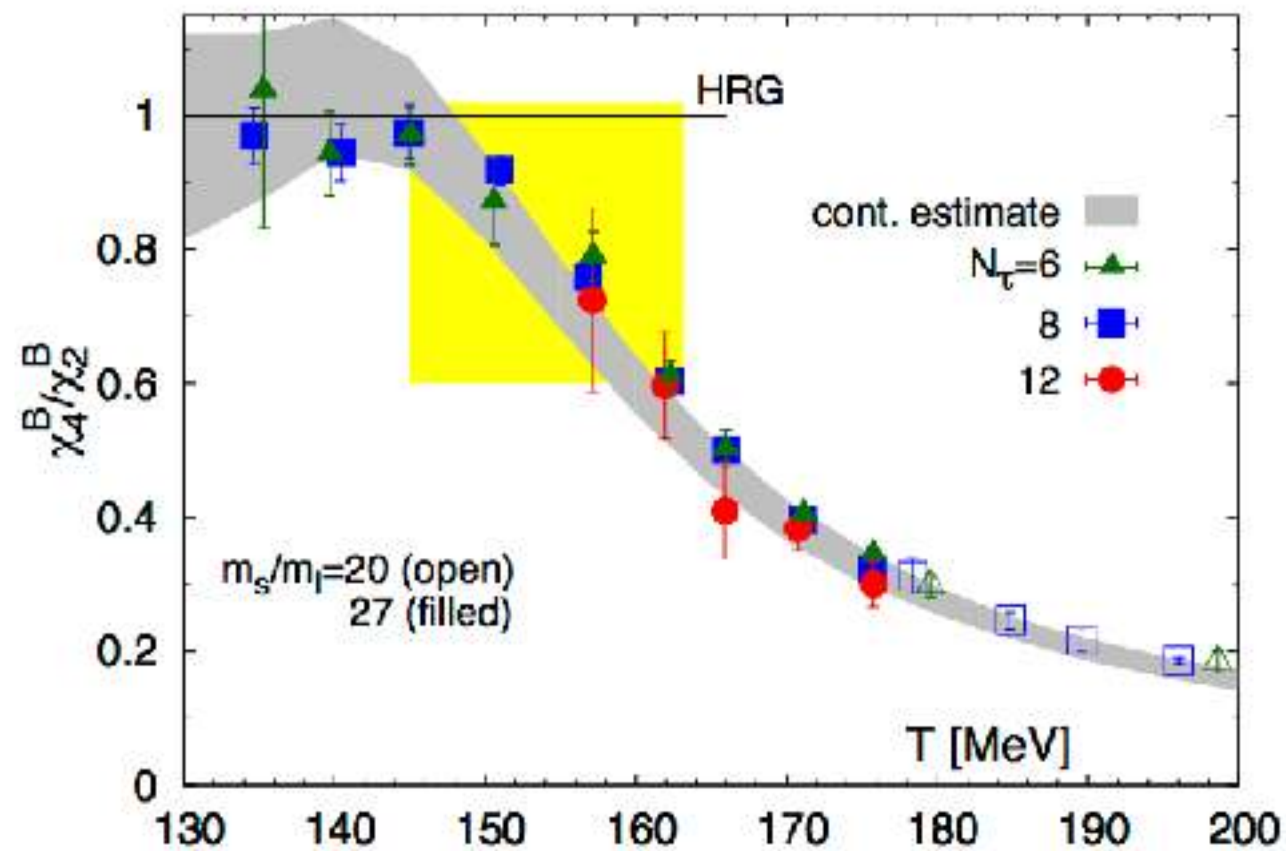

- We used the exponential formalism to calculate 2nd and 4th order QNS, and the linear formalism from the 6th order onwards.
- Our measurements were carried out on 50-100,000 configurations for each temperature with 1500 random sources for D_1 and 500 random sources for the higher-order traces on each configuration.

Coupling the chemical potential μ

- Straightforward coupling of μ to the quark matrix leads to μ^2/a^2 divergences.

- Coupling μ exponentially (so that it appears as part of the fourth component of the vector potential) gets rid of these divergences [Hasenfratz & Karsch (1984)]. However now unlike in the continuum, not only the first but all higher derivatives of the quark matrix are also non-zero. The additional terms act like counterterms that serve to cancel the divergence.

- Alternatively, one may couple μ linearly but to the conserved current [Gavai & Sharma (2010)]. Now divergences do arise and need to be subtracted. However these only appear at 0^{th}, 2^{nd} and 4^{th} orders. Higher orders are still divergence free.

- Moreover, since μ is coupled linearly, all derivatives except the first are zero.

Linear vs Exponential μ

- Coupling μ non-linearly gives rise to all possible derivative terms. The number of terms rises rapidly with increasing order.

- For e.g. in the exponential formalism, at sixth order one has the following traces viz.

$$
\begin{aligned}
\frac{\partial^6 \ln \det M}{\partial \mu^6} = {} & \mathrm{Tr}\left(M^{-1}\frac{\partial^6 M}{\partial \mu^6}\right) - 6\,\mathrm{Tr}\left(M^{-1}\frac{\partial M}{\partial \mu}M^{-1}\frac{\partial^5 M}{\partial \mu^5}\right) - 15\,\mathrm{Tr}\left(M^{-1}\frac{\partial^2 M}{\partial \mu^2}M^{-1}\frac{\partial^4 M}{\partial \mu^4}\right) - 10\,\mathrm{Tr}\left(M^{-1}\frac{\partial^3 M}{\partial \mu^3}M^{-1}\frac{\partial^3 M}{\partial \mu^3}\right) \\
& + 30\,\mathrm{Tr}\left(M^{-1}\frac{\partial M}{\partial \mu}M^{-1}\frac{\partial M}{\partial \mu}M^{-1}\frac{\partial^4 M}{\partial \mu^4}\right) + 60\,\mathrm{Tr}\left(M^{-1}\frac{\partial M}{\partial \mu}M^{-1}\frac{\partial^2 M}{\partial \mu^2}M^{-1}\frac{\partial^3 M}{\partial \mu^3}\right) \\
& + 60\,\mathrm{Tr}\left(M^{-1}\frac{\partial^2 M}{\partial \mu^2}M^{-1}\frac{\partial M}{\partial \mu}M^{-1}\frac{\partial^3 M}{\partial \mu^3}\right) + 30\,\mathrm{Tr}\left(M^{-1}\frac{\partial^2 M}{\partial \mu^2}M^{-1}\frac{\partial^2 M}{\partial \mu^2}M^{-1}\frac{\partial^2 M}{\partial \mu^2}\right) \\
& - 120\,\mathrm{Tr}\left(M^{-1}\frac{\partial M}{\partial \mu}M^{-1}\frac{\partial M}{\partial \mu}M^{-1}\frac{\partial M}{\partial \mu}M^{-1}\frac{\partial^3 M}{\partial \mu^3}\right) - 180\,\mathrm{Tr}\left(M^{-1}\frac{\partial M}{\partial \mu}M^{-1}\frac{\partial M}{\partial \mu}M^{-1}\frac{\partial^2 M}{\partial \mu^2}M^{-1}\frac{\partial^2 M}{\partial \mu^2}\right) \\
& - 90\,\mathrm{Tr}\left(M^{-1}\frac{\partial M}{\partial \mu}M^{-1}\frac{\partial^2 M}{\partial \mu^2}M^{-1}\frac{\partial M}{\partial \mu}M^{-1}\frac{\partial^2 M}{\partial \mu^2}\right) + 360\,\mathrm{Tr}\left(M^{-1}\frac{\partial M}{\partial \mu}M^{-1}\frac{\partial M}{\partial \mu}M^{-1}\frac{\partial M}{\partial \mu}M^{-1}\frac{\partial M}{\partial \mu}M^{-1}\frac{\partial^2 M}{\partial \mu^2}\right) \\
& - 120\,\mathrm{Tr}\left(M^{-1}\frac{\partial M}{\partial \mu}M^{-1}\frac{\partial M}{\partial \mu}M^{-1}\frac{\partial M}{\partial \mu}M^{-1}\frac{\partial M}{\partial \mu}M^{-1}\frac{\partial M}{\partial \mu}M^{-1}\frac{\partial M}{\partial \mu}\right).
\end{aligned}
$$

Linear vs Exponential μ

- Coupling μ non-linearly gives rise to all possible derivative terms. The number of terms rises rapidly with increasing order.

- By contrast, if μ is coupled linearly, all terms with second and higher derivatives of μ are zero.

= 0

$$
\begin{aligned}
\frac{\partial^6 \ln \det M}{\partial \mu^6} = {} & \mathrm{Tr}\left(M^{-1}\frac{\partial^6 M}{\partial \mu^6}\right) - 6\,\mathrm{Tr}\left(M^{-1}\frac{\partial M}{\partial \mu}M^{-1}\frac{\partial^5 M}{\partial \mu^5}\right) - 15\,\mathrm{Tr}\left(M^{-1}\frac{\partial^2 M}{\partial \mu^2}M^{-1}\frac{\partial^4 M}{\partial \mu^4}\right) - 10\,\mathrm{Tr}\left(M^{-1}\frac{\partial^3 M}{\partial \mu^3}M^{-1}\frac{\partial^3 M}{\partial \mu^3}\right) \\
& + 30\,\mathrm{Tr}\left(M^{-1}\frac{\partial M}{\partial \mu}M^{-1}\frac{\partial M}{\partial \mu}M^{-1}\frac{\partial^4 M}{\partial \mu^4}\right) + 60\,\mathrm{Tr}\left(M^{-1}\frac{\partial M}{\partial \mu}M^{-1}\frac{\partial^2 M}{\partial \mu^2}M^{-1}\frac{\partial^3 M}{\partial \mu^3}\right) \\
& + 60\,\mathrm{Tr}\left(M^{-1}\frac{\partial^2 M}{\partial \mu^2}M^{-1}\frac{\partial M}{\partial \mu}M^{-1}\frac{\partial^3 M}{\partial \mu^3}\right) + 30\,\mathrm{Tr}\left(M^{-1}\frac{\partial^2 M}{\partial \mu^2}M^{-1}\frac{\partial^2 M}{\partial \mu^2}M^{-1}\frac{\partial^2 M}{\partial \mu^2}\right) \\
& - 120\,\mathrm{Tr}\left(M^{-1}\frac{\partial M}{\partial \mu}M^{-1}\frac{\partial M}{\partial \mu}M^{-1}\frac{\partial M}{\partial \mu}M^{-1}\frac{\partial^3 M}{\partial \mu^3}\right) - 180\,\mathrm{Tr}\left(M^{-1}\frac{\partial M}{\partial \mu}M^{-1}\frac{\partial M}{\partial \mu}M^{-1}\frac{\partial^2 M}{\partial \mu^2}M^{-1}\frac{\partial^2 M}{\partial \mu^2}\right) \\
& - 90\,\mathrm{Tr}\left(M^{-1}\frac{\partial M}{\partial \mu}M^{-1}\frac{\partial^2 M}{\partial \mu^2}M^{-1}\frac{\partial M}{\partial \mu}M^{-1}\frac{\partial^2 M}{\partial \mu^2}\right) + 360\,\mathrm{Tr}\left(M^{-1}\frac{\partial M}{\partial \mu}M^{-1}\frac{\partial M}{\partial \mu}M^{-1}\frac{\partial M}{\partial \mu}M^{-1}\frac{\partial M}{\partial \mu}M^{-1}\frac{\partial^2 M}{\partial \mu^2}\right) \\
& - 120\,\mathrm{Tr}\left(M^{-1}\frac{\partial M}{\partial \mu}M^{-1}\frac{\partial M}{\partial \mu}M^{-1}\frac{\partial M}{\partial \mu}M^{-1}\frac{\partial M}{\partial \mu}M^{-1}\frac{\partial M}{\partial \mu}M^{-1}\frac{\partial M}{\partial \mu}\right).
\end{aligned}
$$

Linear vs Exponential μ

- Thus one only needs N matrix inversions at N^{th} order. By comparison, in the exponential case one needs around 20 matrix inversions at sixth order.
- Since matrix inversion is the most expensive part of the calculation, this results in a huge gain at higher orders.

= 0

$$
\begin{aligned}
\frac{\partial^6 \ln \det M}{\partial \mu^6} = {} & \mathrm{Tr}\left(M^{-1}\frac{\partial^6 M}{\partial \mu^6}\right) - 6\,\mathrm{Tr}\left(M^{-1}\frac{\partial M}{\partial \mu}M^{-1}\frac{\partial^5 M}{\partial \mu^5}\right) - 15\,\mathrm{Tr}\left(M^{-1}\frac{\partial^2 M}{\partial \mu^2}M^{-1}\frac{\partial^4 M}{\partial \mu^4}\right) - 10\,\mathrm{Tr}\left(M^{-1}\frac{\partial^3 M}{\partial \mu^3}M^{-1}\frac{\partial^3 M}{\partial \mu^3}\right) \\
& + 30\,\mathrm{Tr}\left(M^{-1}\frac{\partial M}{\partial \mu}M^{-1}\frac{\partial M}{\partial \mu}M^{-1}\frac{\partial^4 M}{\partial \mu^4}\right) + 60\,\mathrm{Tr}\left(M^{-1}\frac{\partial M}{\partial \mu}M^{-1}\frac{\partial^2 M}{\partial \mu^2}M^{-1}\frac{\partial^3 M}{\partial \mu^3}\right) \\
& + 60\,\mathrm{Tr}\left(M^{-1}\frac{\partial^2 M}{\partial \mu^2}M^{-1}\frac{\partial M}{\partial \mu}M^{-1}\frac{\partial^3 M}{\partial \mu^3}\right) + 30\,\mathrm{Tr}\left(M^{-1}\frac{\partial^2 M}{\partial \mu^2}M^{-1}\frac{\partial^2 M}{\partial \mu^2}M^{-1}\frac{\partial^2 M}{\partial \mu^2}\right) \\
& - 120\,\mathrm{Tr}\left(M^{-1}\frac{\partial M}{\partial \mu}M^{-1}\frac{\partial M}{\partial \mu}M^{-1}\frac{\partial M}{\partial \mu}M^{-1}\frac{\partial^3 M}{\partial \mu^3}\right) - 180\,\mathrm{Tr}\left(M^{-1}\frac{\partial M}{\partial \mu}M^{-1}\frac{\partial M}{\partial \mu}M^{-1}\frac{\partial^2 M}{\partial \mu^2}M^{-1}\frac{\partial^2 M}{\partial \mu^2}\right) \\
& - 90\,\mathrm{Tr}\left(M^{-1}\frac{\partial M}{\partial \mu}M^{-1}\frac{\partial^2 M}{\partial \mu^2}M^{-1}\frac{\partial M}{\partial \mu}M^{-1}\frac{\partial^2 M}{\partial \mu^2}\right) + 360\,\mathrm{Tr}\left(M^{-1}\frac{\partial M}{\partial \mu}M^{-1}\frac{\partial M}{\partial \mu}M^{-1}\frac{\partial M}{\partial \mu}M^{-1}\frac{\partial M}{\partial \mu}M^{-1}\frac{\partial^2 M}{\partial \mu^2}\right) \\
& - 120\,\mathrm{Tr}\left(M^{-1}\frac{\partial M}{\partial \mu}M^{-1}\frac{\partial M}{\partial \mu}M^{-1}\frac{\partial M}{\partial \mu}M^{-1}\frac{\partial M}{\partial \mu}M^{-1}\frac{\partial M}{\partial \mu}M^{-1}\frac{\partial M}{\partial \mu}\right).
\end{aligned}
$$

Strangeness neutrality and initial conditions in heavy-ion collisions

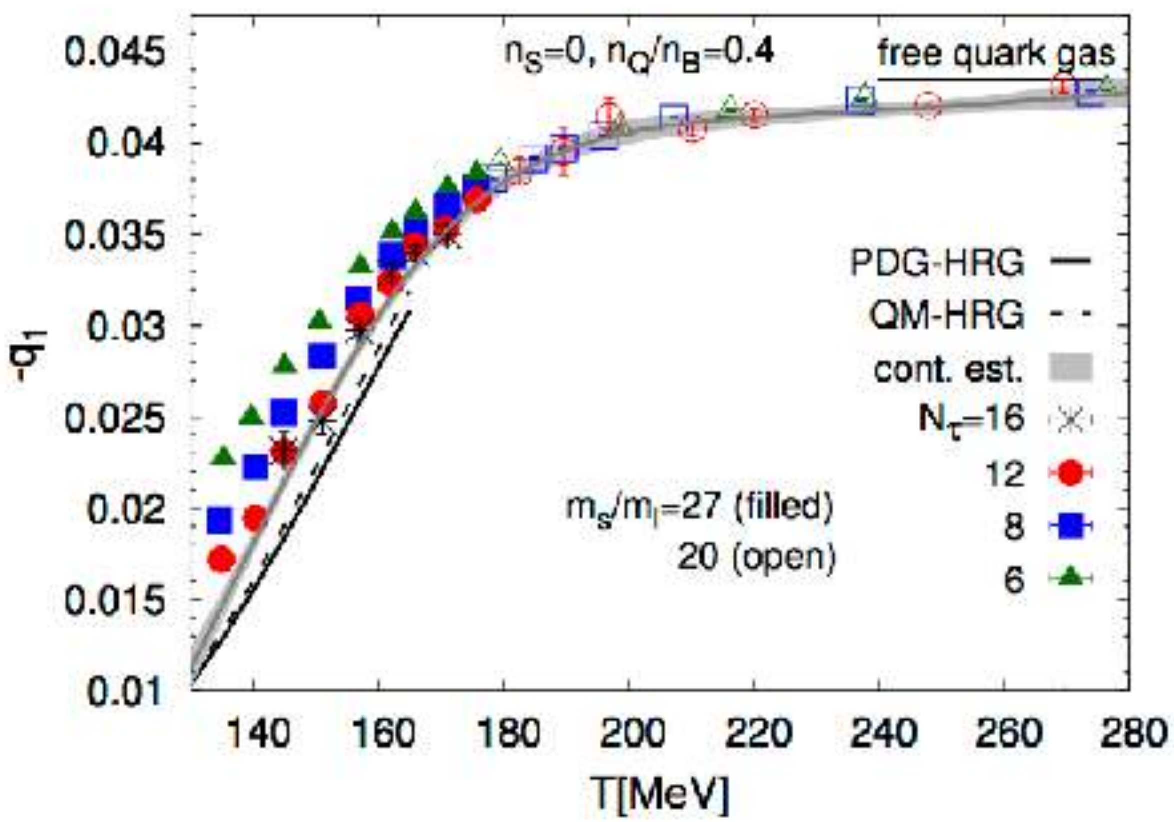

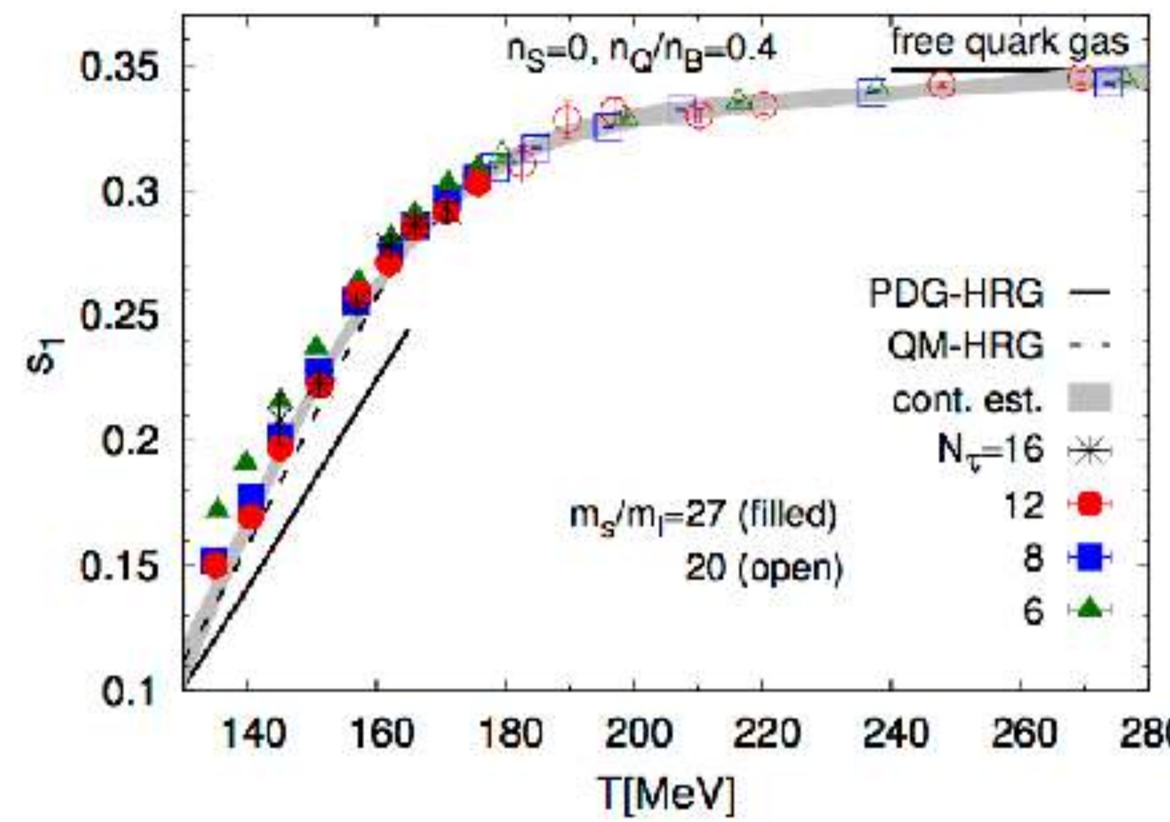

The initial conditions in a heavy-ion collision are i) $n_S = 0$ (net strangeness zero), and ii) n_Q/n_B = const. (fixed proton-to-neutron ratio).

These conditions imply that μ_Q and μ_S are nonzero whenever μ_B is. Using the QNS, they can be determined order-by-order in μ_B.

Results: Ratios and differences of cumulants

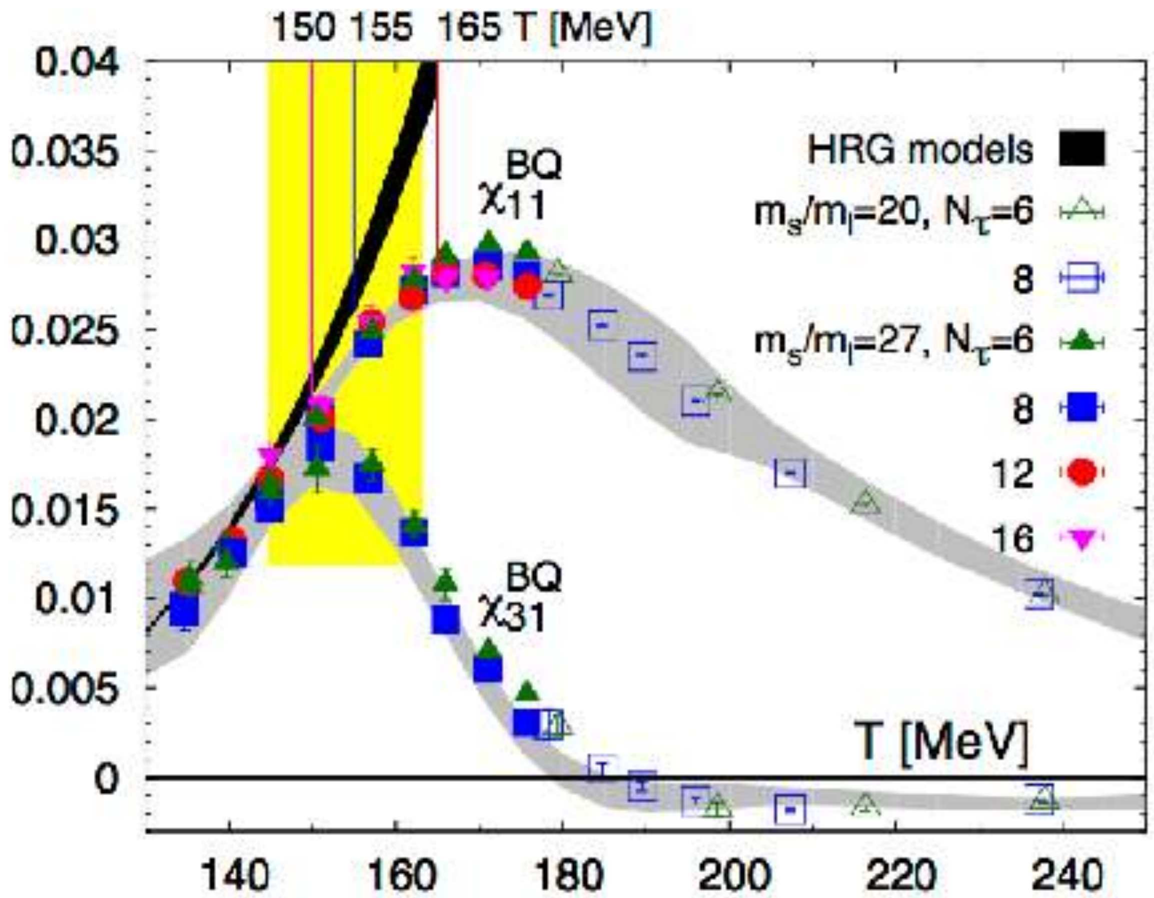

- Our results for the QNS agree with Hadron Resonance Gas (HRG) predictions below the chiral phase transition temperature T_c=154 +/- 9 MeV.

Figures from the CPOD 2016 talk by F. Karsch [arXiv:1703.06702].

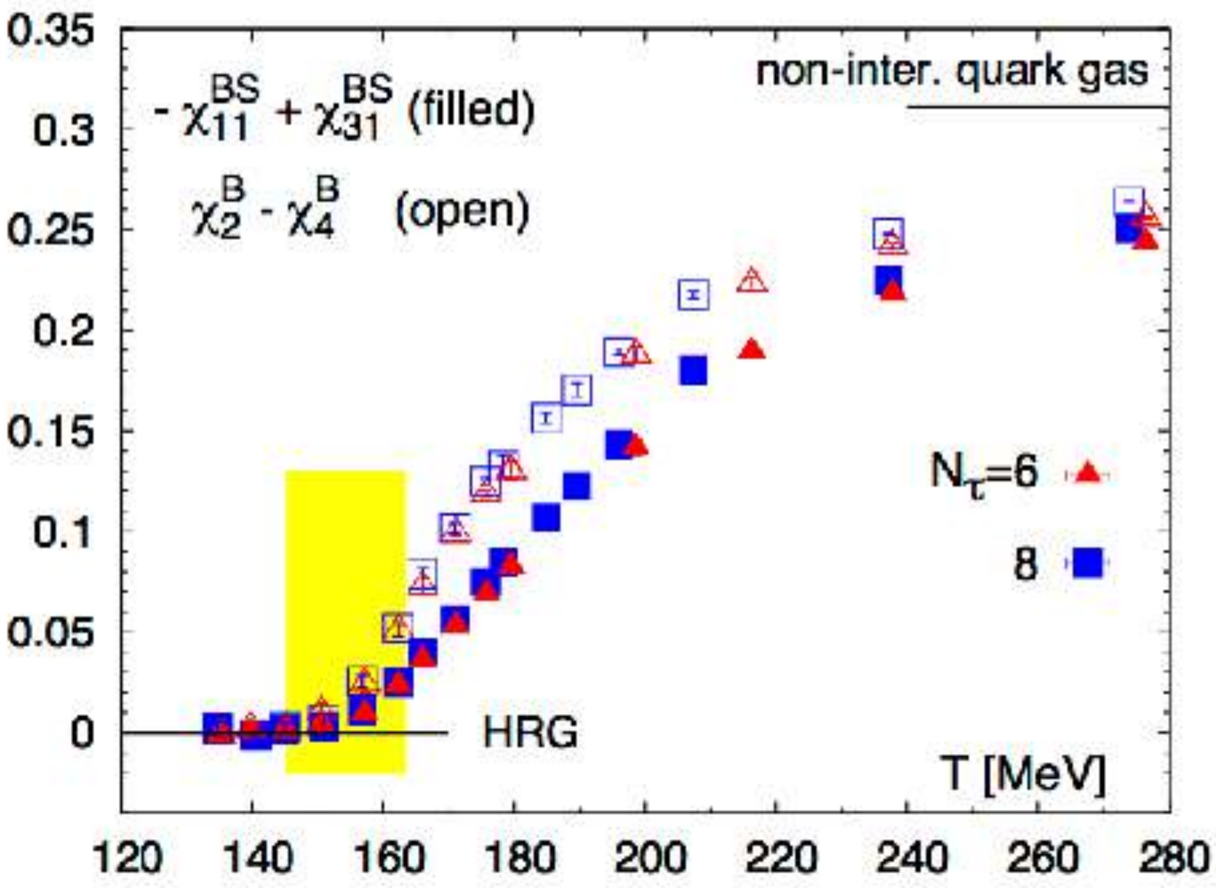

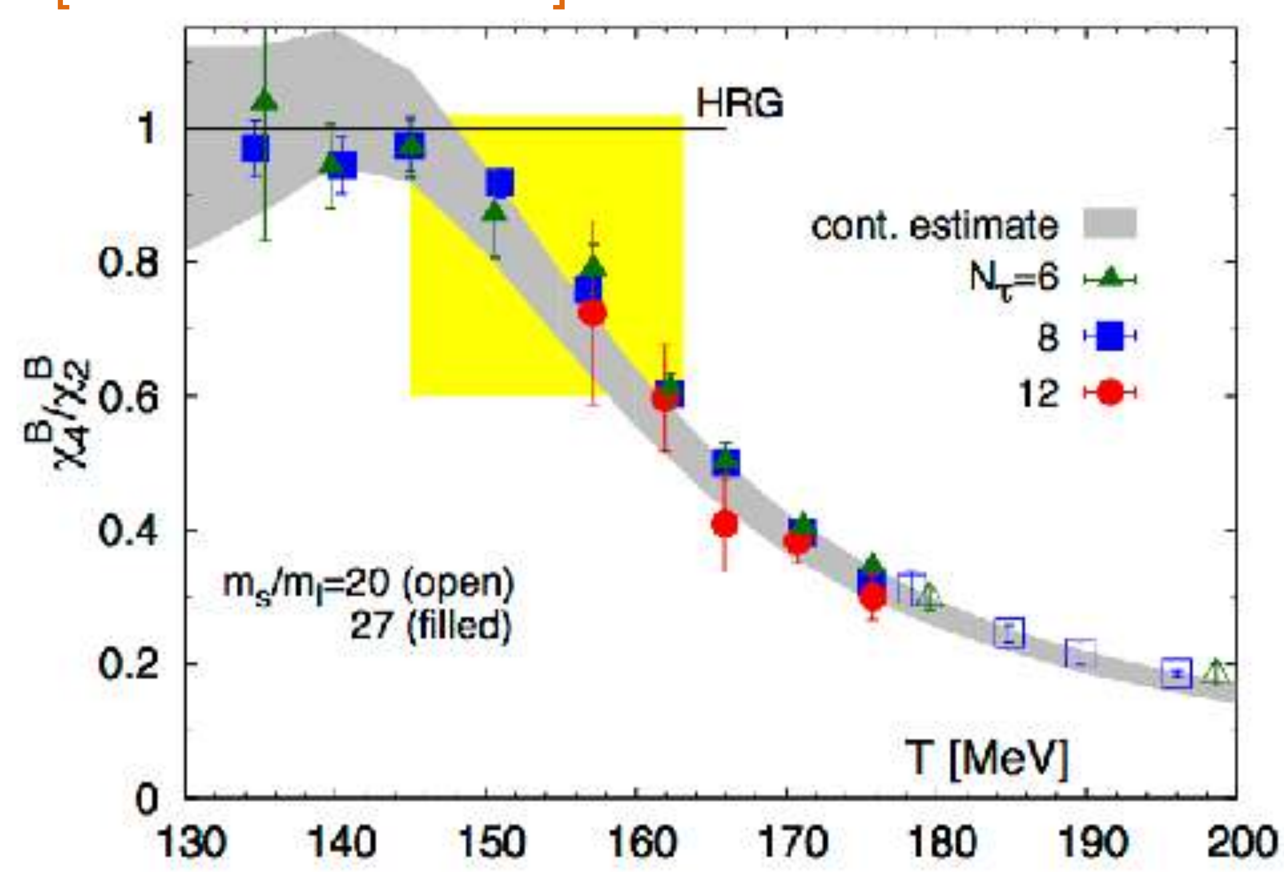

HRG comparison: Strangeness sector

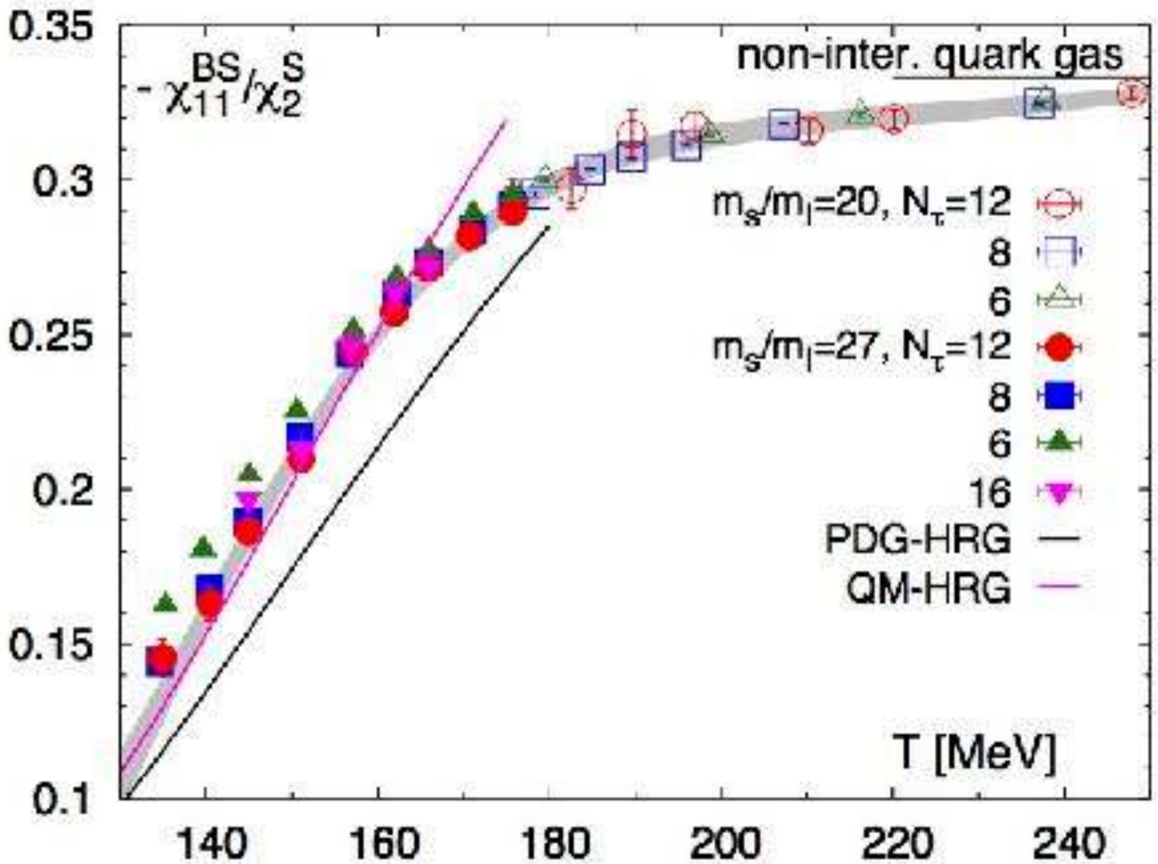

- Apparent deviations from HRG in the strange sector disappear if additional, as yet unobserved, strange hadrons (as predicted by various Quark Models, for e.g.) are taken into account.

- Excluded-volume HRG models have also been proposed to explain such differences. However we find that such models cannot reproduce our lattice results uniformly [See talk by F. Karsch at this year's Quark Matter conference [arXiv: 1706.01620]].

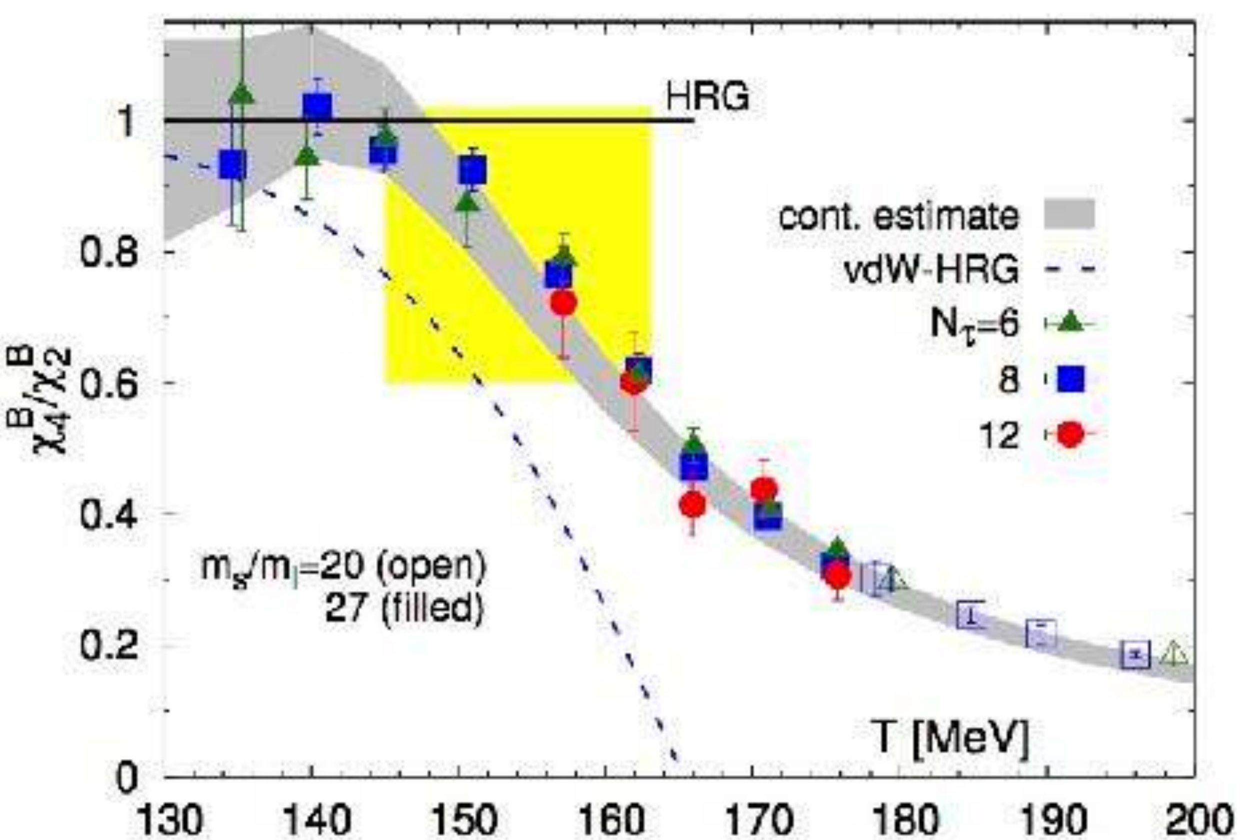

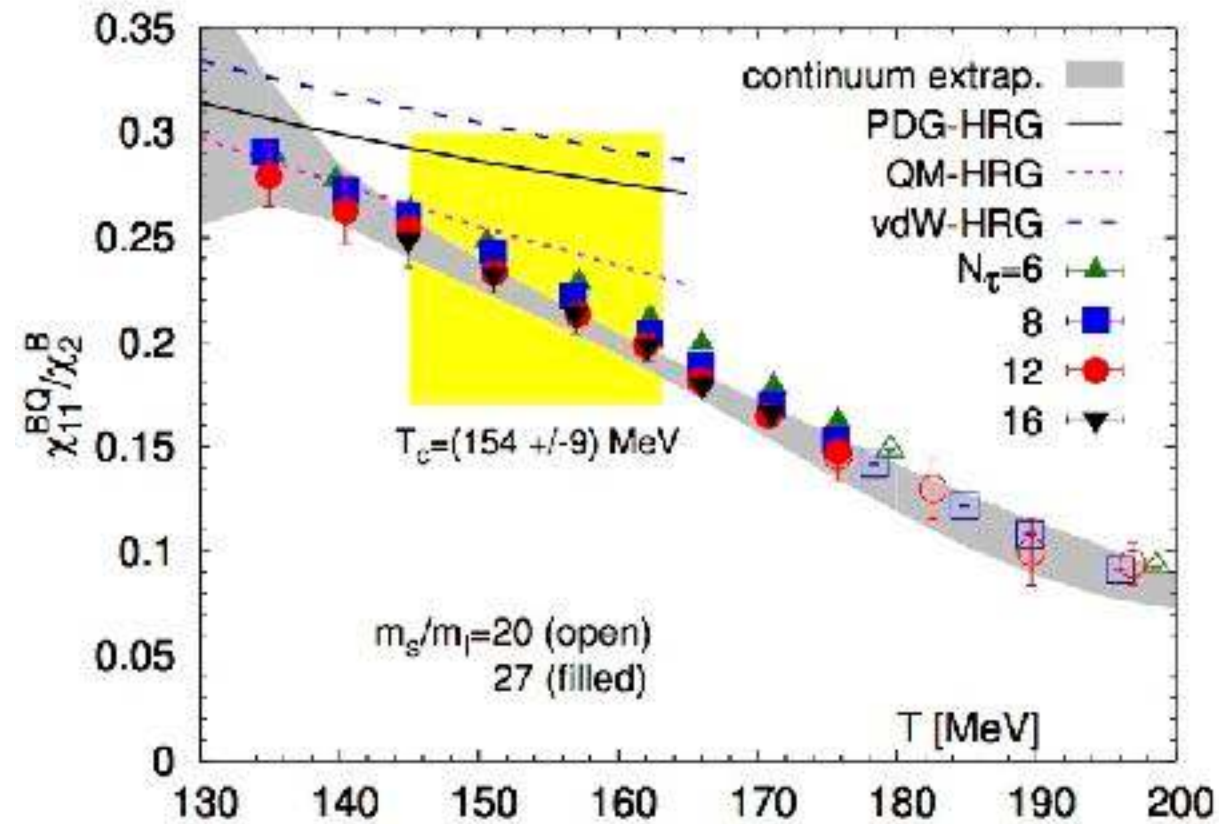

Extracting Freeze-out Parameters

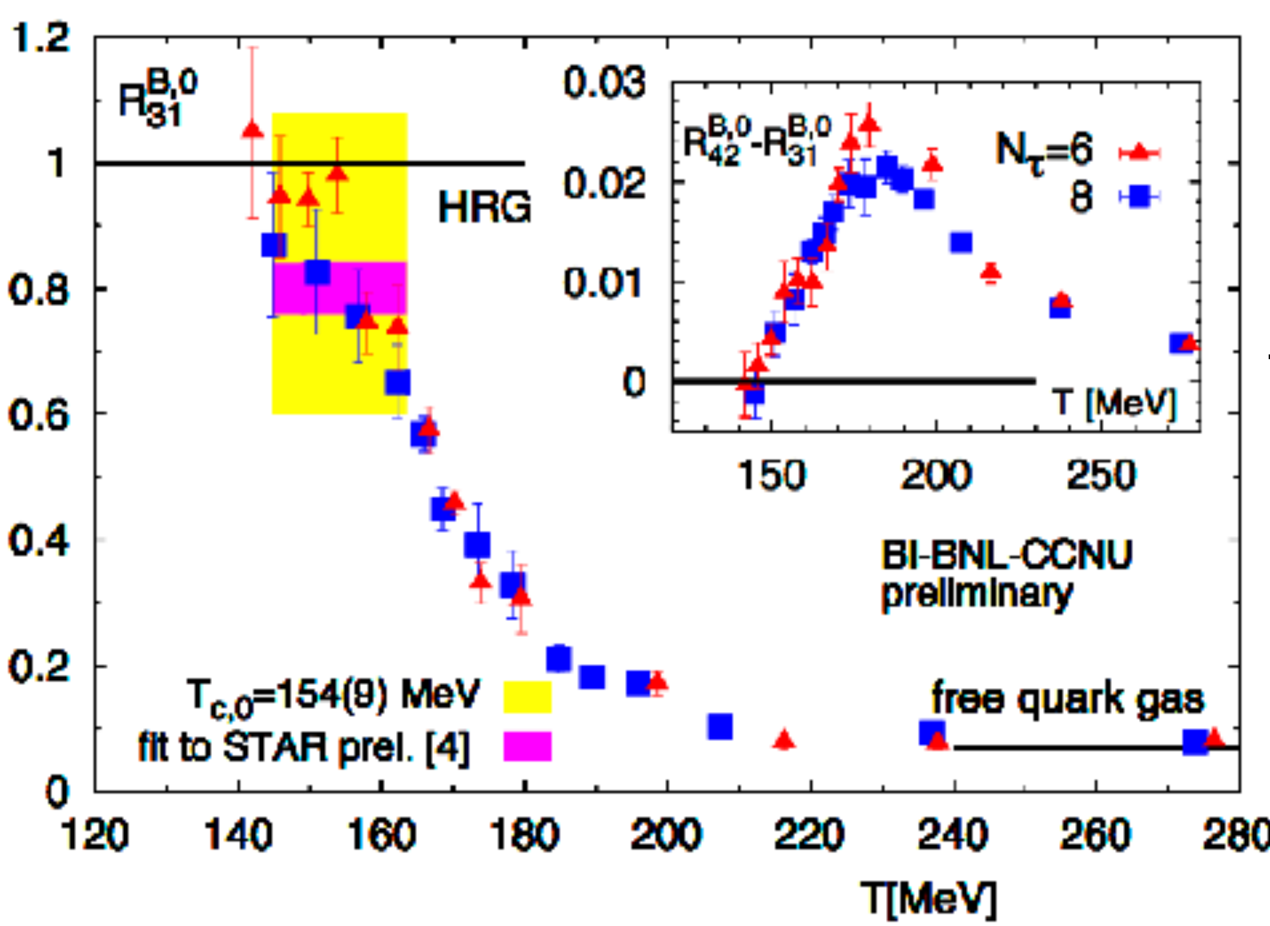

It is possible to obtain T^f and $\mu_B{}^f$ by comparing the observed ratios of fluctuations to lattice QCD results [A. Bazavov *et al.*, Phys. Rev. **D93** no.1, 014512 (2016) and F. Karsch, QM2015 and Nucl. Phys. A956, 352 (2016)].

Identical to the m_1 and m_3 ratios of R.Gavai and S.Gupta (Phys. Lett. **B696**, 459 (2011)).

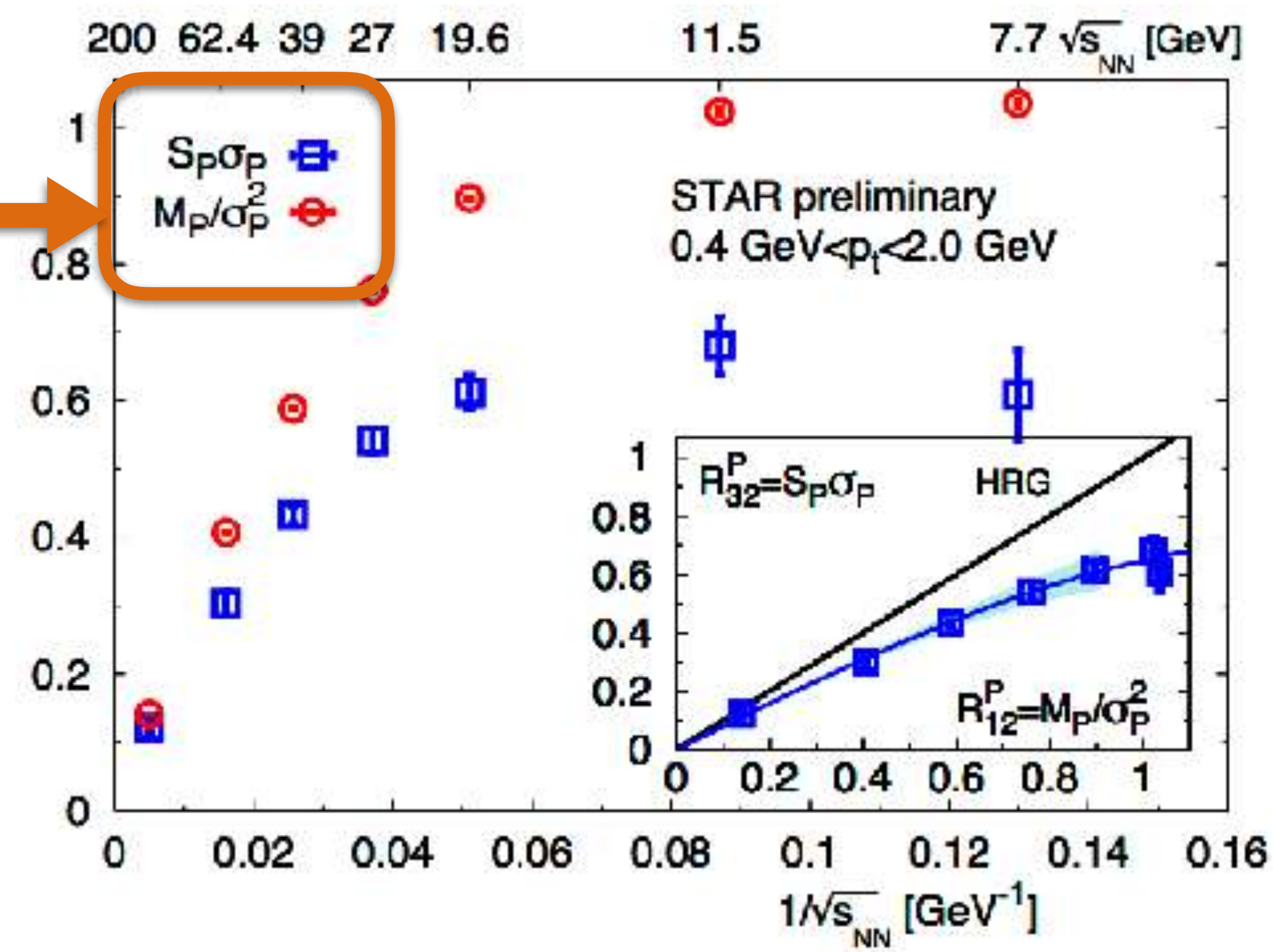

Certainly, the beam energy dependence of cumulant ratios is reproducible by considering a finite-μ_B expansion of the cumulants

Corrections to the pressure

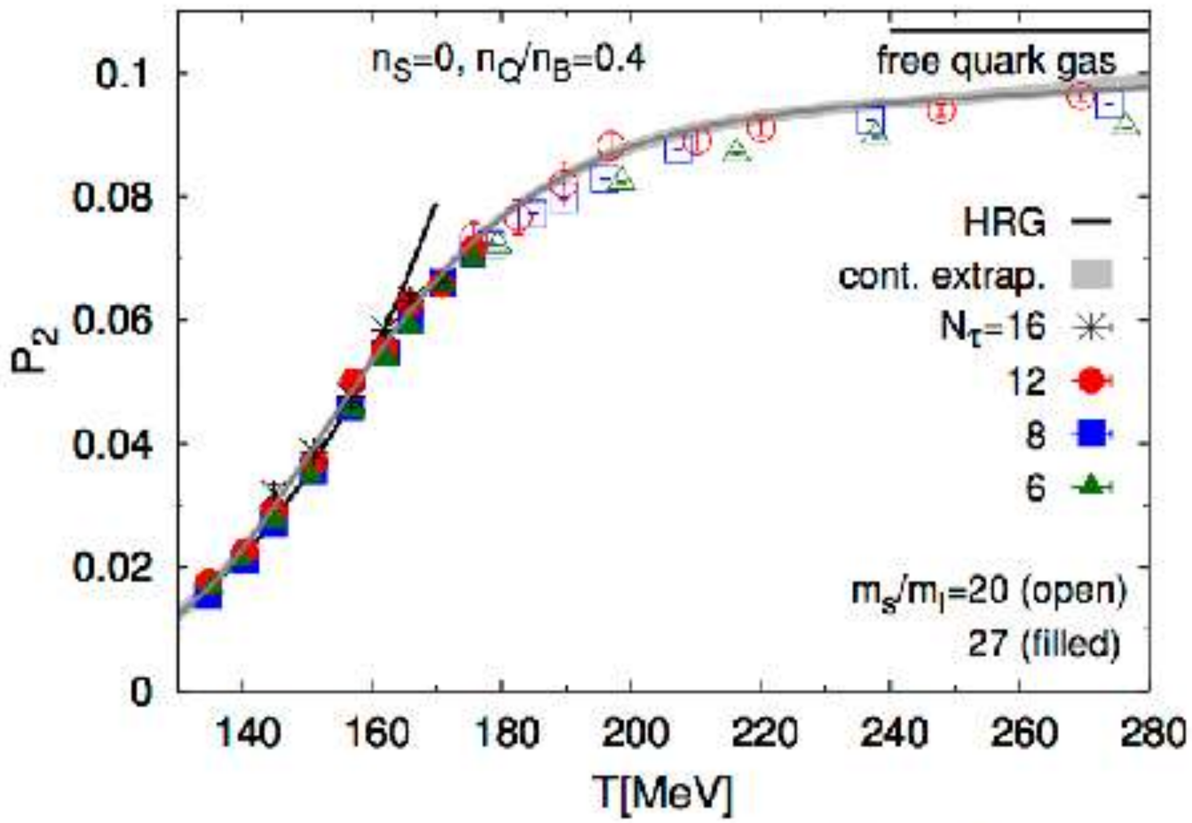

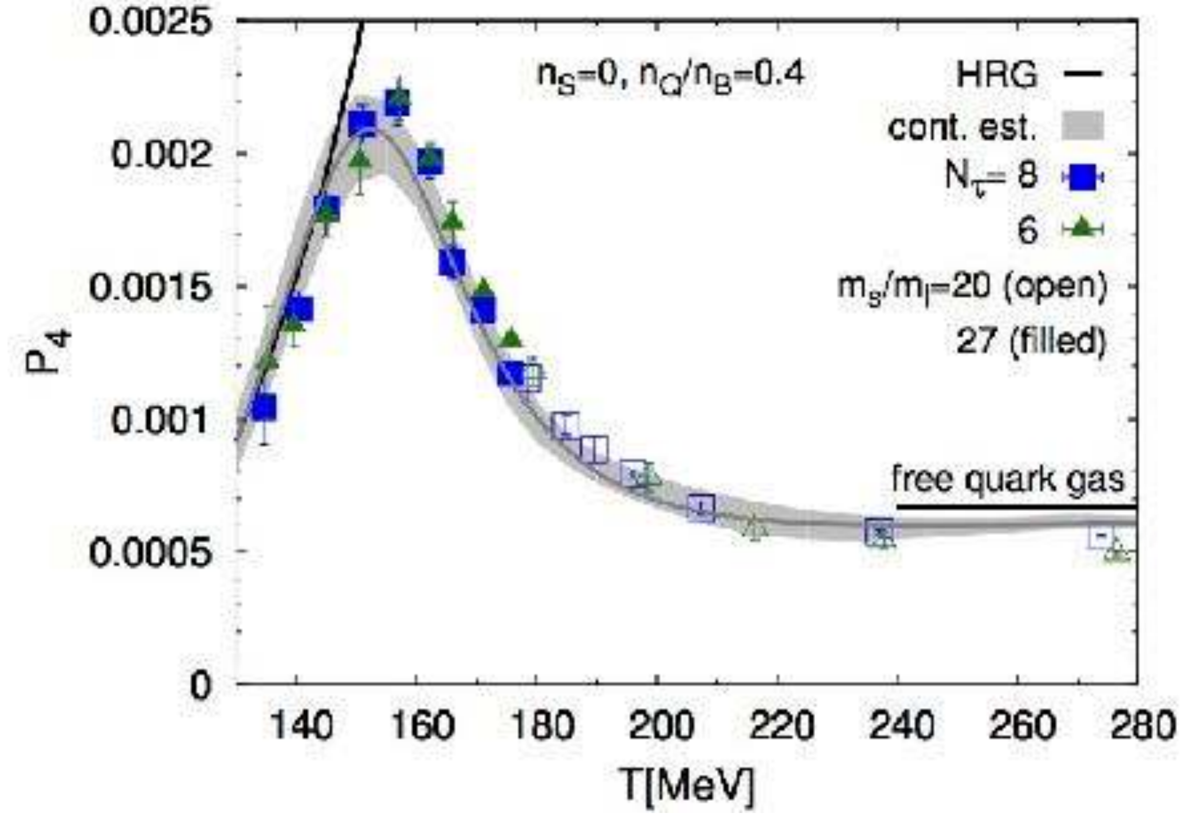

These corrections are to be added to the 0th order EoS [Bielefeld-BNL-CCNU, Phys. Rev. D90, 054503 (2014)]

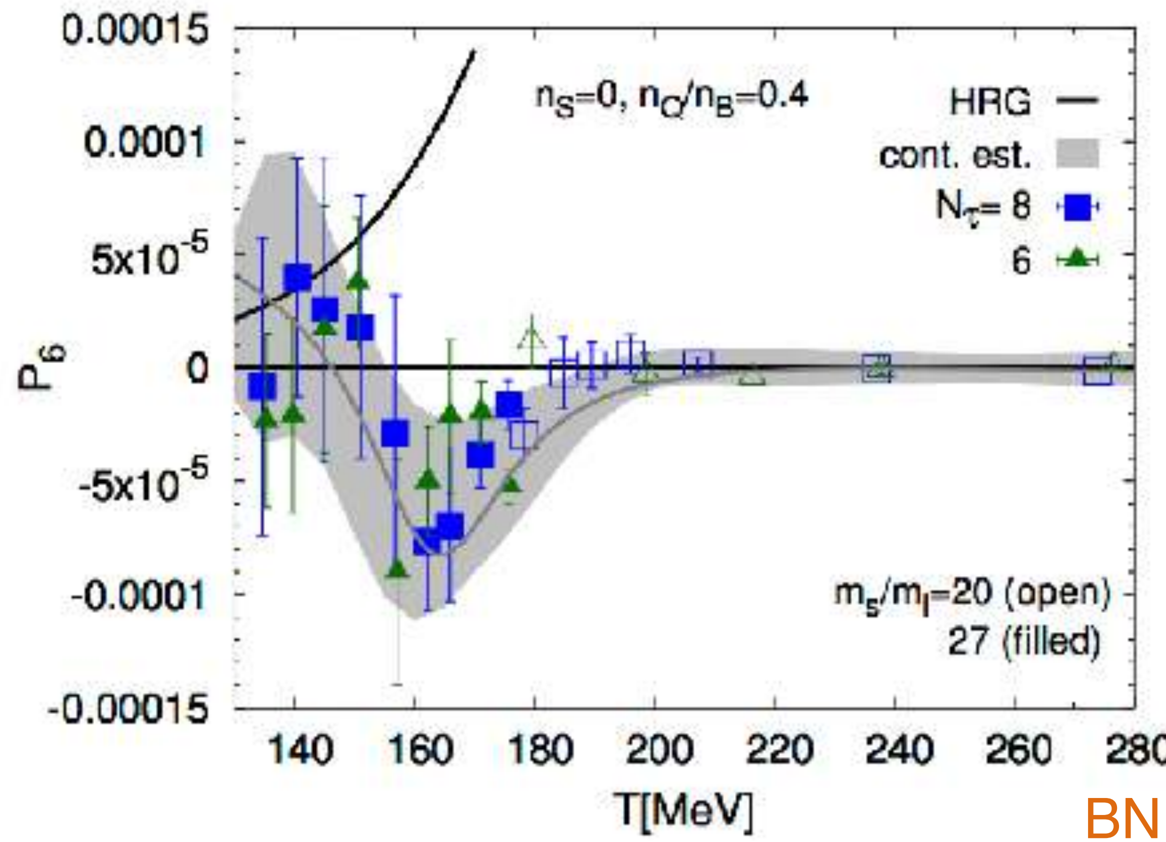

Shapes can be qualitatively understood as due to the 2nd order O(4) transition in the chiral limit.

BNL-Bielefeld-CCNU, Phys. Rev. **D86**, 054504 (2017)

Pressure, energy and entropy

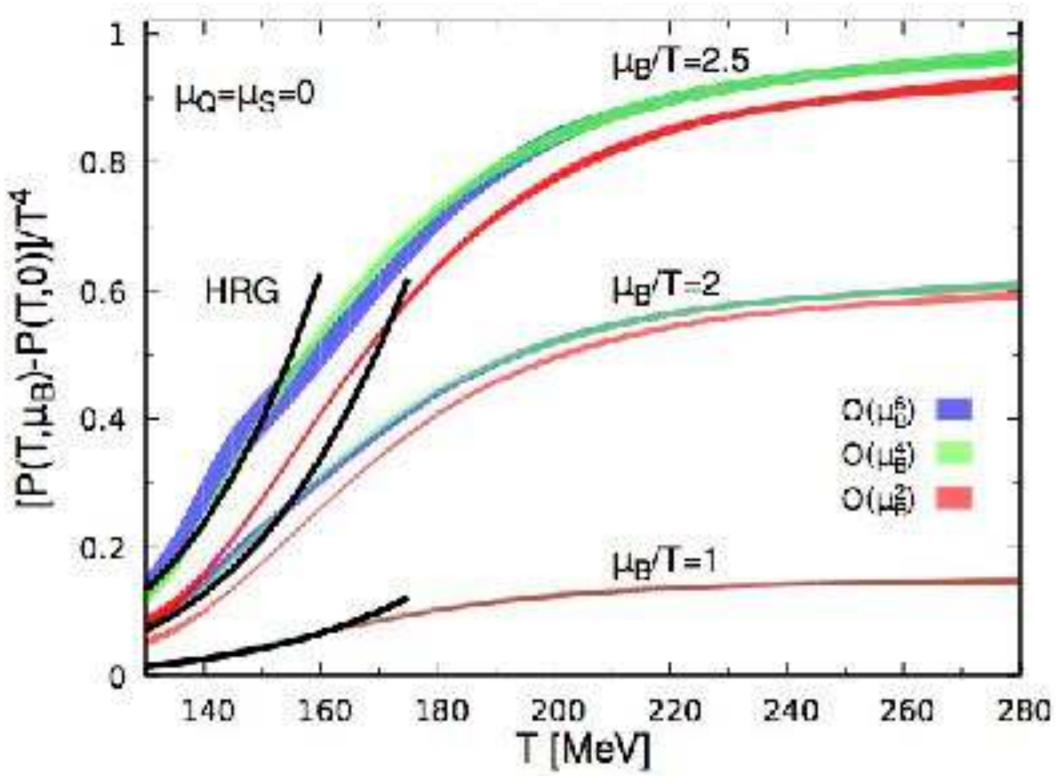

6th-order contributions start to become visible beyond $\mu_B/T = 2$.

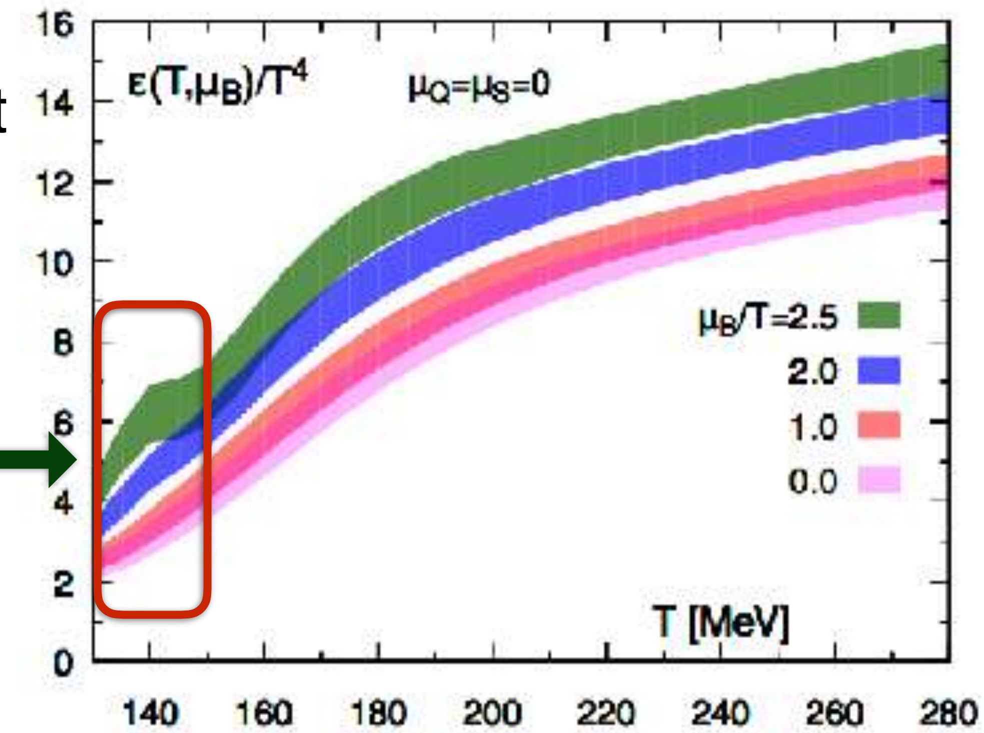

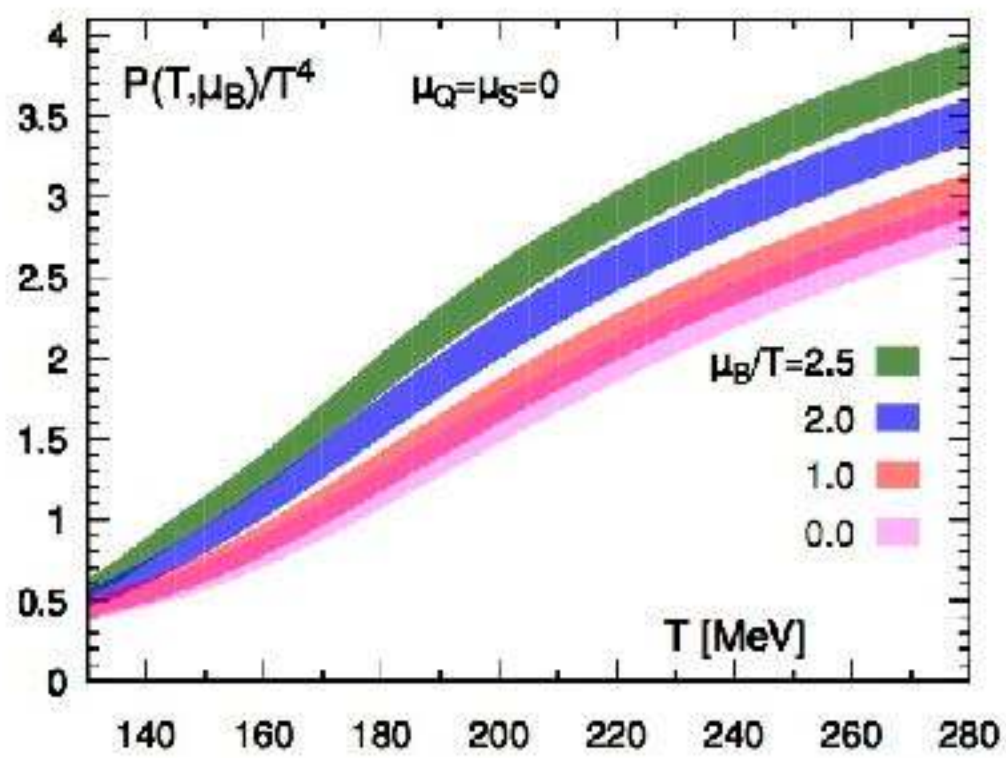

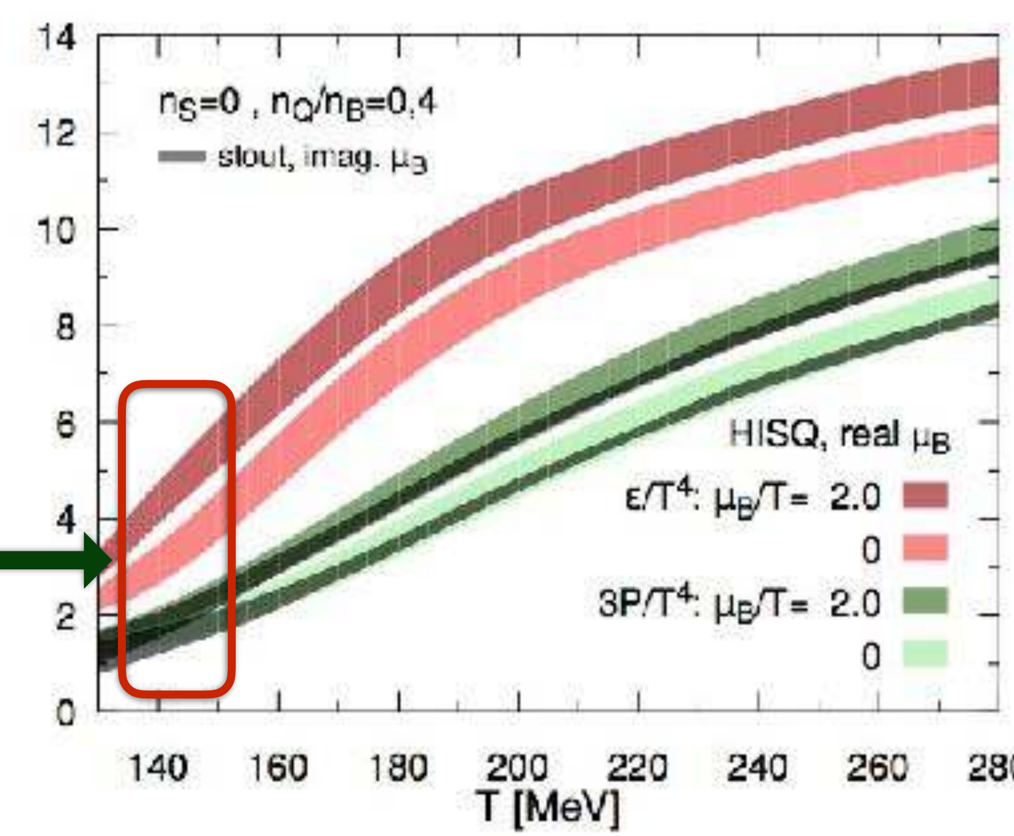

Lines of constant physics and the curvature of the freeze-out line

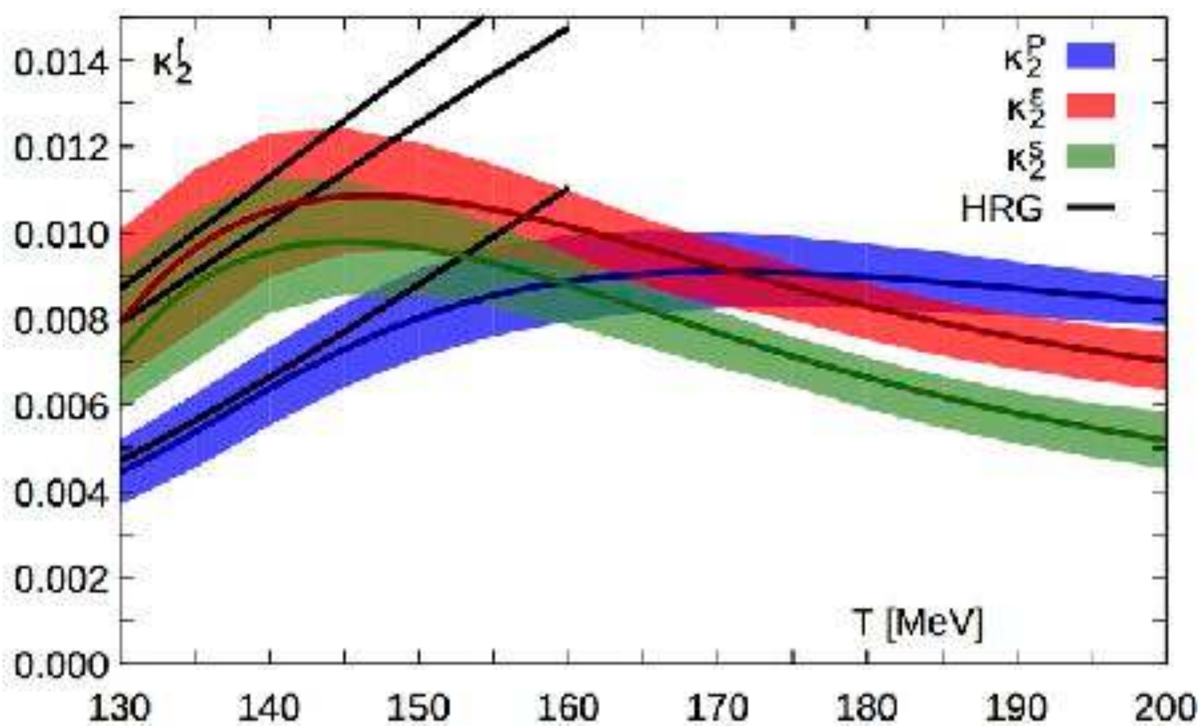

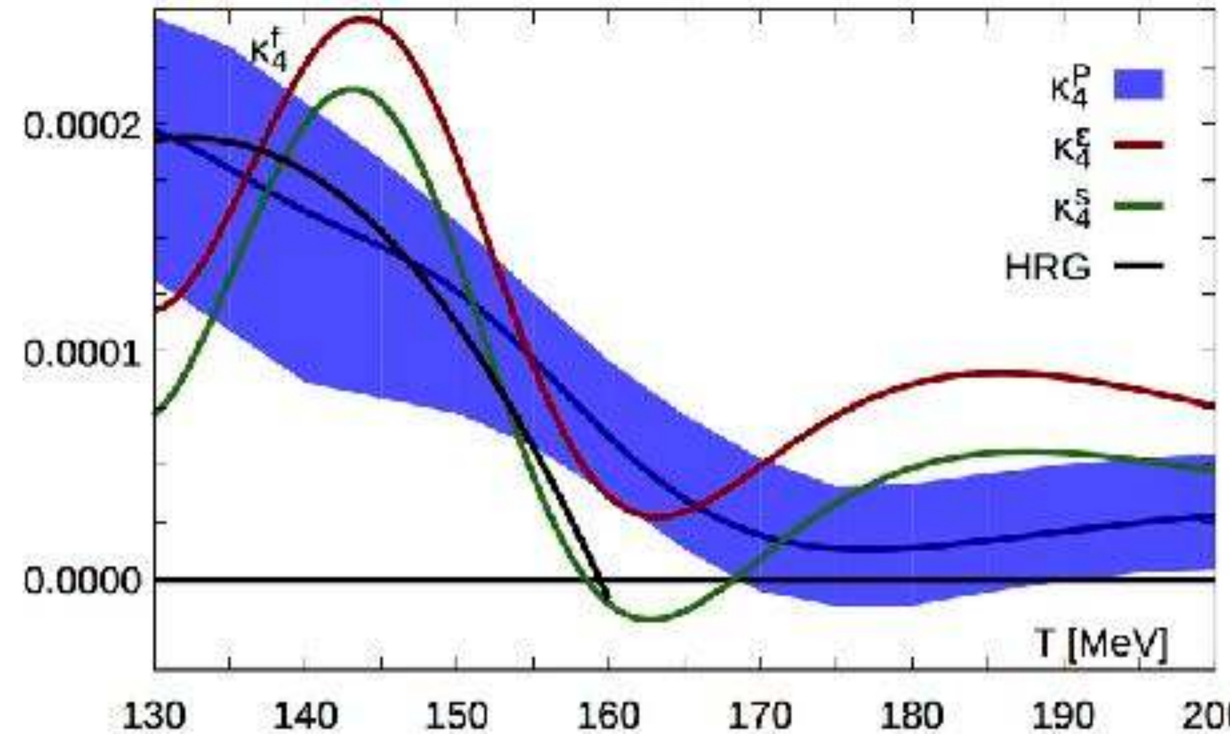

Lines of constant p, σ or ε are curves in the T-μ_B plane. For small μ_B, we can parametrize: $T(\mu_B) = T_0 + \kappa_2(\mu_B/T)^2 + \kappa_4(\mu_B/T)^4 + \ldots$

We determine κ_2 and κ_4 from our 2nd and 4th-order Taylor expansions. κ_4 is smaller than κ_2 by an order of magnitude. Our current statistics do not permit an accurate determination of κ_6.

Lines of constant physics and the curvature of the freeze-out line

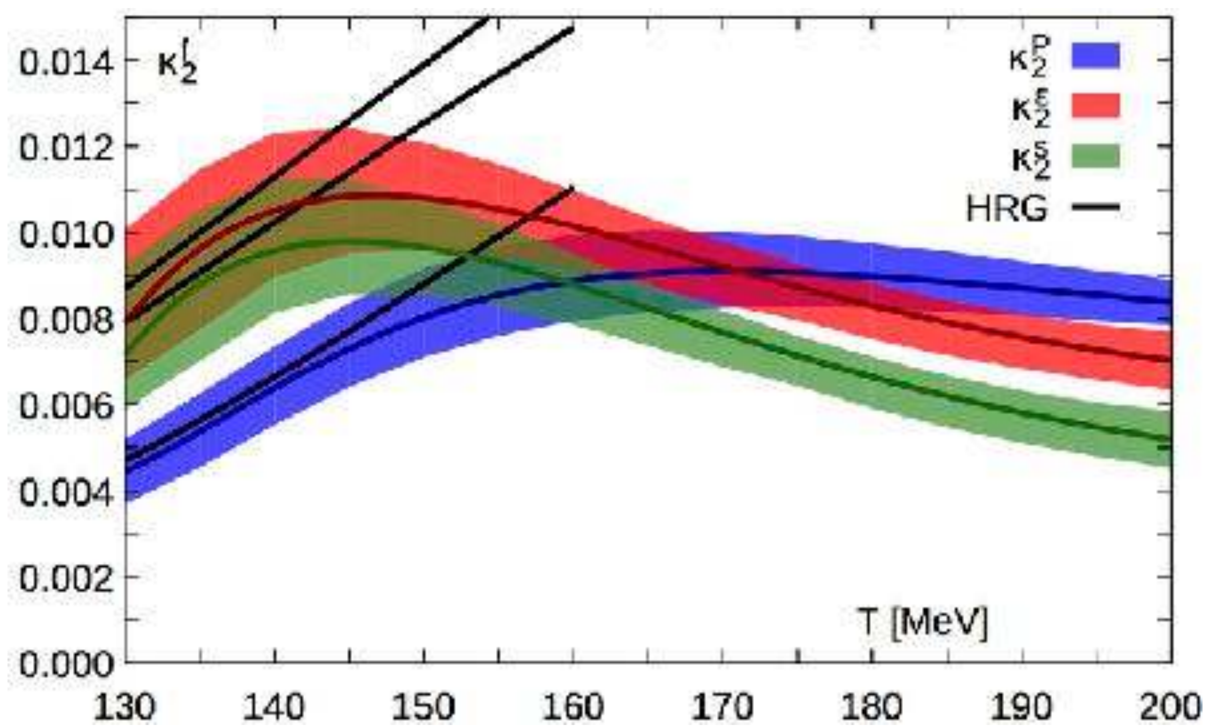

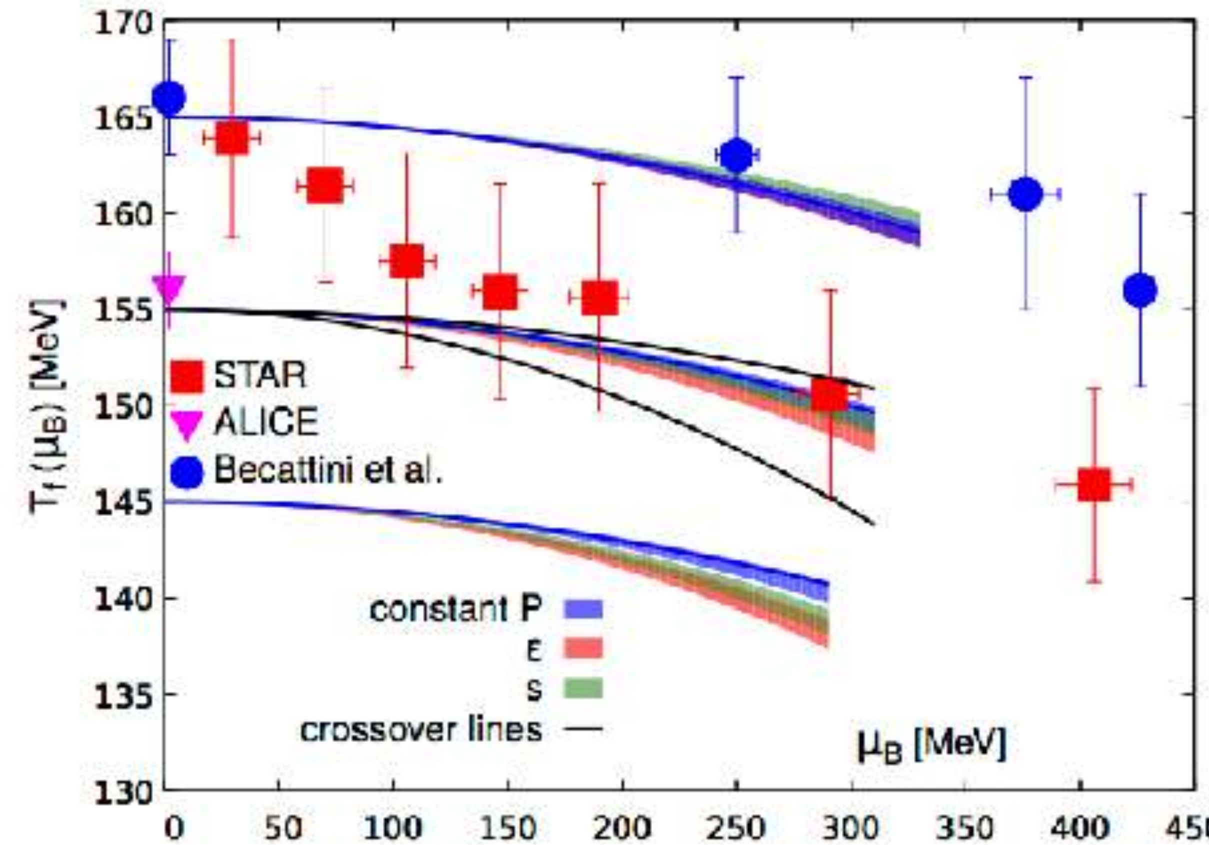

Phenomenologically, freeze-out has been conjectured to occur along such lines of constant ε or σ [Cleymans and Redlich 1999].

For T between 145 and 165 MeV, $0.0064 <= \kappa_2^p <= 0.0101$ and $0.0087 <= \kappa_2^\varepsilon <= 0.012$ [S. Sharma, QM2017]. This is in agreement with estimates for the curvature of the line of the chiral transition temperature [BNL-Bielefeld 2010; BW 2012, 2015; D'Elia *et al*. 2015; Cea *et al*. 2015].

Searching for the QCD Critical Point

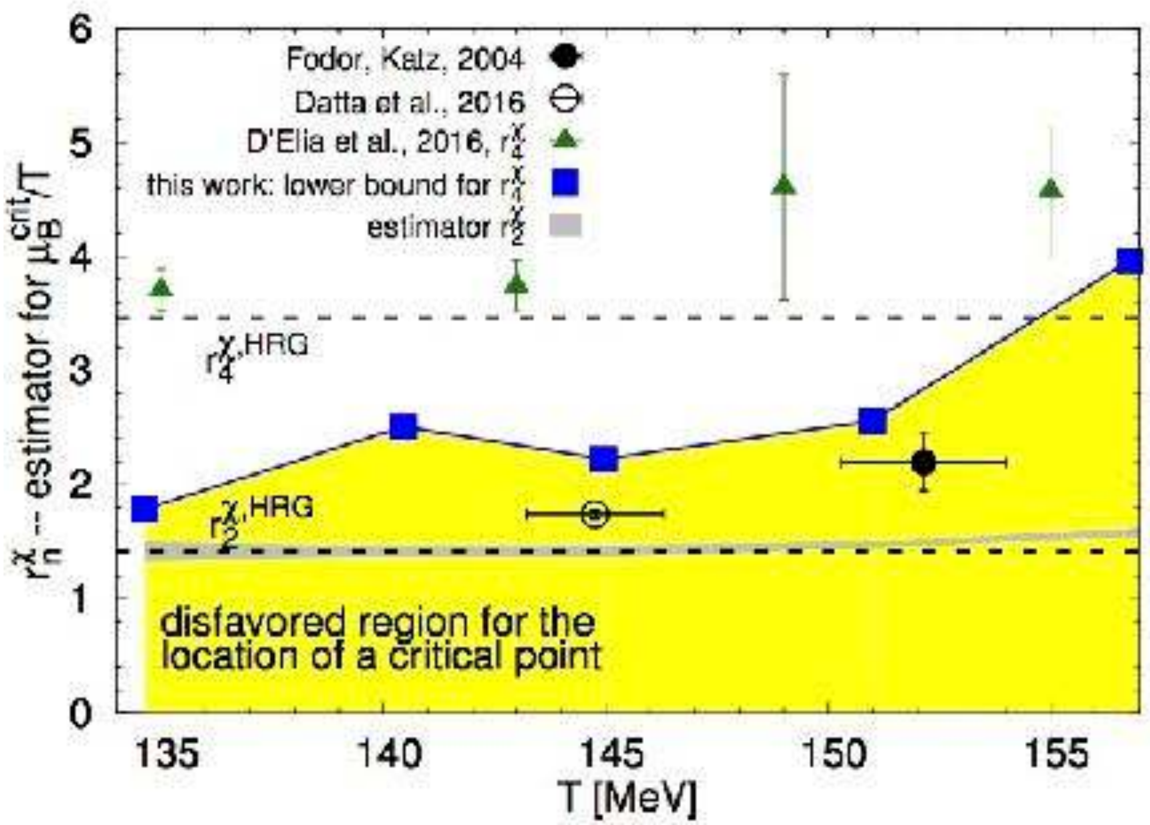

[Phys. Rev. D95, no. 5, 054504 (2017)]

Our calculations seem to indicate that our expansions are under control for $\mu_B/T <= 2$. That is, the corrections strictly obey $P_2 >> P_4 >> P_6 >> \ldots$

Every Taylor series has a radius of convergence (which could be infinite), which is also the distance to the nearest singularity. In our case, this singularity would be the QCD critical point.

Close to the singularity, contributions from different orders start to become equal, leading to a breakdown of the expansion. This distance can be estimated from the formula:

$$\rho = \lim_{n\to\infty} \sqrt{\frac{P_n}{P_{n+2}}}$$

Searching for the QCD Critical Point

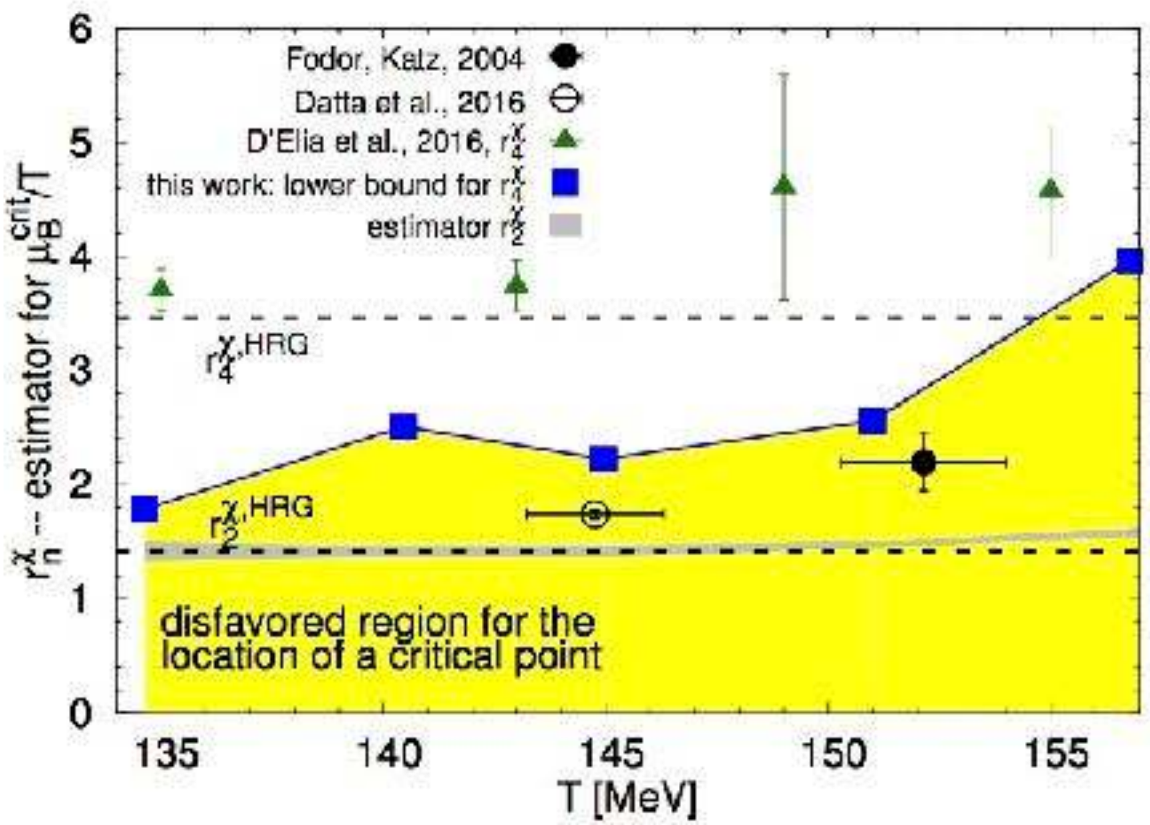

[Phys. Rev. D95, no. 5, 054504 (2017)]

It has also been pointed out that the baryon number susceptibility χ_2^B diverges at the critical point. The Taylor expansion for χ_2^B is given by:

$$\chi_2^B(\hat{\mu}) = \chi_2^B + \frac{\chi_4^B}{2}\left(\frac{\mu_B}{T}\right)^2 + \frac{\chi_6^B}{24}\left(\frac{\mu_B}{T}\right)^4 + \dots$$

Similar to the pressure, the radius of convergence can be estimated by taking

$$\rho_\chi = \lim_{n\to\infty} r_{2n}^\chi = \lim_{n\to\infty}\sqrt{\frac{2n(2n-1)\chi_{2n}^B}{\chi_{2n+2}^B}}$$

Our results seem to suggest that ρ_χ for 135 MeV <= T <= 160 MeV is greater than 1.8 – 2. This conclusion was drawn from the behavior of the first two ratios r_2 and r_4.

Conclusions

- We have presented our results for a 6th order equation of state based on a high-statistics Taylor expansion in lattice QCD.
- We find that our expansion is under control for baryochemical potentials $\mu_B/T \le 2$, and possibly for slightly larger potentials as well.
- This also places limits on the possible location of the QCD critical point in the T-μ_B phase diagram.
- We are also able to use our expansions to determine various other observables of interest, such as the freeze out parameters as well as lines of constant physics (LCP).